Icelandic
Meteorological Office

Veðurstofa Íslands

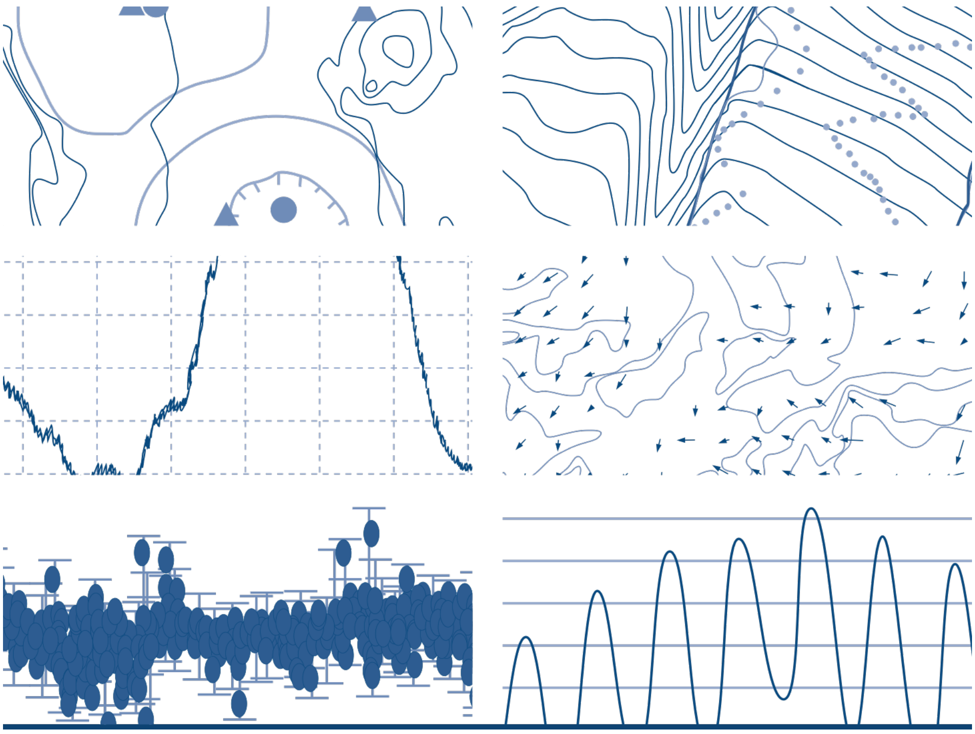

Evaluation of two delineation methods for regional flood frequency analysis in northern Iceland

Philippe Crochet

Report

VÍ 2012-013

Icelandic
Meteorological Office

Veðurstofa Íslands

Evaluation of two delineation methods for regional flood frequency analysis in northern Iceland

Philippe Crochet, Icelandic Met Office

Report

Veðurstofa Íslands
Bústaðavegur 7–9
150 Reykjavík

+354 522 60 00
vedur@vedur.is

VÍ 2012-013
ISSN 1670-8261

Keypage

Veðurstofa Íslands

Report no.:	Date:	ISSN:	Public ☒ Restricted ☐
VÍ 2012-013	October 2012	1670-8261	Provision:

Report title / including subtitle Evaluation of two delineation methods for regional flood frequency analysis in northern Iceland	**No. of copies:** 20 **Pages:** 55 **Managing director:** Jórunn Harðardóttir
Author(s): Philippe Crochet	**Project manager:** Philippe Crochet **Project number:** 4812
Project phase:	**Case number:** 2012-373

Report contracted for:
Vegagerðin (Icelandic Road Administration)

Prepared in cooperation with:

Summary:

The goal of this study is to present a regional flood frequency analysis for estimating flood return periods at ungauged and poorly gauged catchments. This information is usually required for the design and management of structures such as bridges, dams and reservoirs. The method involves two major steps, i) the delineation of a set of hydrologically homogeneous watersheds with respect to extreme flood statistics, which constitute a "region" and ii) a regional estimation method which transfers the regional flood frequency distribution calculated with streamflow data from the gauged sites, to ungauged or poorly gauged sites, after proper rescaling. In a previous study, geographic regions were arbitrarily defined. Two objective regionalisation techniques are now evaluated for delineating automatically homogeneous regions, namely a hierarchical clustering approach and the so-called region of influence approach. The results indicate that the two objective delineation techniques look promising and should be used rather than a geographic delineation as they allow for similar or better results in a rational and more objective manner.

Keywords: Iceland, flood, regional flood frequency analysis	**Managing director's signature:** Jórunn Harðard. **Project manager's signature:** **Reviewed by:** Tinna Þórarinsdóttir, SG

Contents

1 Introduction

Flood frequency analysis is used by hydrologists to estimate the return period associated with a flood of a given magnitude. This information is often needed for the design of various structures such as bridges and dams and in hydrological applications such as reservoir management and analyses of dam safety. In practise, this information is often required at locations where streamflow series are either not long enough to allow for a robust calculation of the flood frequency distribution and the estimation of floods of long return periods, or where no data are available at all. In such a case, regional flood frequency analysis offers a solution to this problem and has widely been used (Stedinger *et al.*, 1992; GREHYS, 1996a, 1996b; Jingyi *and* Hall, 2004; Das *and* Cunnane, 2011; Malekinezhad *et al.*, 2011a and 2011b). The idea is to compensate for the lack of temporal data by spatial data, taken within a region with similar flood behaviour. The underlying assumption is that flood data within the homogeneous region are drawn from the same frequency distribution, apart from a scaling factor. The method involves two major steps, i) the delineation of a set of hydrologically homogeneous watersheds, which is performed by selecting gauging stations that are assumed to constitute a region with sufficient homogeneity regarding extreme flow characteristics and ii) a regional estimation method which transfers the regional flood frequency distribution at each site of interest after proper rescaling. Recently, the usefulness of such a method was evaluated for ten catchments in northern Iceland (Crochet, 2012a). The homogeneous regions were simply defined according to the geographic proximity of the different catchments. In this study, this methodology is further developed and two automatic delineation techniques are tested, namely the agglomerative hierarchical clustering approach and the so-called region of influence approach (Burn, 1990a, 1990b). This report is organized as follows. Section 2 presents the data used in the study. Section 3 describes the regional flood frequency analysis and the two delineation techniques. Section 4 presents an inter-comparison of the different strategies for estimating instantaneous flood frequency distribution at poorly gauged and ungauged catchments. Finally, Section 5 concludes this report.

2 Data

2.1 River basins

The same ten watersheds used in Crochet (2012a) have been used in this study. Five of them are located in northern Iceland, in the Tröllaskagi region and surroundings and the other five in the West-fjords and surroundings. The catchments boundaries are shown in Fig. 1 with a topographic map. Table 1 summarizes the main physiographic and climatic characteristics. The drainage of the catchment areas varies from 37 km^2 for the smallest to 1096 km^2 for the largest. The mean catchment altitude varies from 403 m a.s.l to 934 m a.s.l with large variations within each watershed. The precipitation climatology is also quite variable, the annual average varies between 813 mm and 3018 mm over the catchments.

Table 1. Main characteristics of river basins.

Gauging station	Rank	Name	Area (km^2)	Mean elevation (m a.s.l)	Minimum elevation (m a.s.l)	Maximum elevation (m a.s.l)	Mean slope (%)	Mean annual precipitation (mm) (1971-2000)
vhm 10	1	Svartá	398	535	67	894	14	813
vhm 51	2	Hjaltadalsá	296	730	78	1265	32	1711
vhm 92	3	Bægisá	39	934	254	1304	41	1928
vhm 200	4	Fnjóská	1096	715	79	1081	17	1312
vhm 45	5	Vatnsdalsá	456	553	121	899	4.4	846
vhm 12	6	Haukadalsá	167	404	54	786	21	1773
vhm 19	7	Dynjandisá	37	529	296	689	10	3018
vhm 38	8	Þverá	43	427	106	521	7	1761
vhm 198	9	Hvalá	195	403	89	576	6	1971
vhm 204	10	Vatnsdalsá	103	456	34	762	13	2937

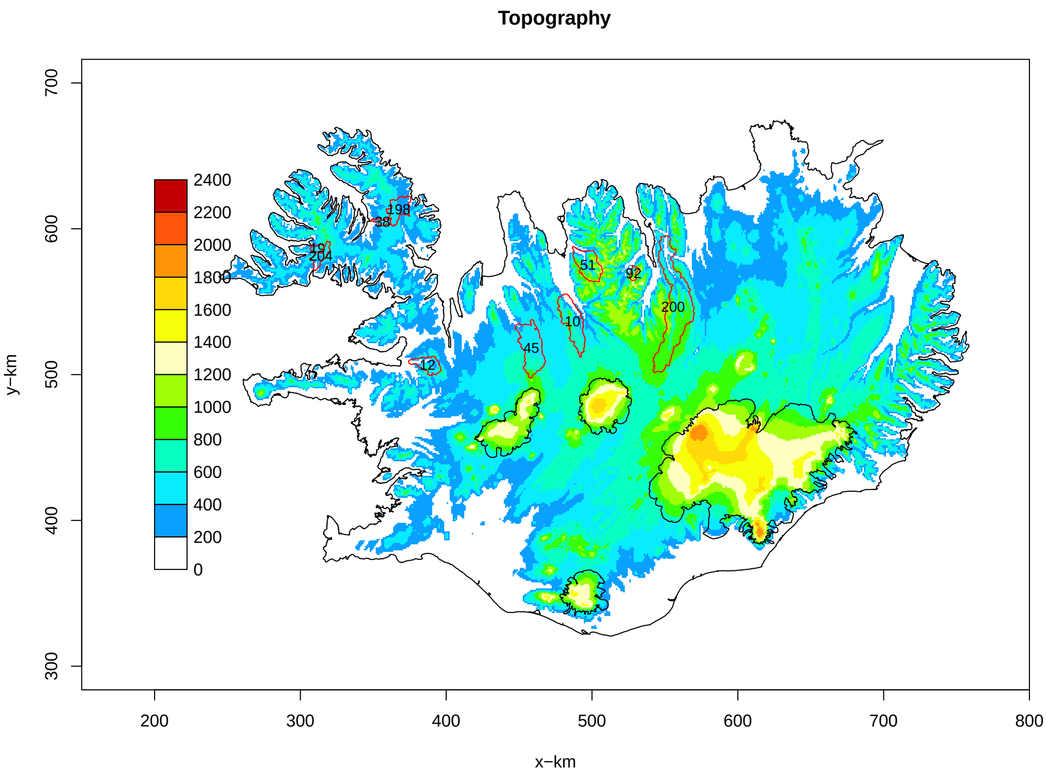

Figure 1. Topography (m a.s.l) and location of catchments.

2.2 Streamflow data

Annual maximum instantaneous discharge series measured at the gauging stations listed in Table 1 were used in this study to represent flood series. These data were extracted from monthly maximum discharge series, considering a water-year that spans 1 Sep. – 31 Aug. Years with more than four missing months were omitted and the longest continuous period with no missing years was selected for each watershed. The dominating flood-generating mechanisms (snowmelt and/or rain) depend on various factors such as the presence of frozen ground, the catchment size and elevation distribution and the precipitation climatology, among others. Some watersheds have most of their annual maximum discharge in late spring or early summer, during snowmelt, but others have annual maxima either in spring, winter or autumn, depending on the year.

3 Regional flood frequency analysis

3.1 General methodology

The regional flood frequency analysis involves two steps, i) the delineation of a homogeneous region (DHR) defined by a group of hydrologically homogeneous watersheds and ii) a regional estimation method (REM). The regional estimation method used here is the so-called index flood method (Dalrymple, 1960) already used and described in Crochet (2012a). The principle of the method is reminded below. The assumption is that the flood frequency distributions of a group of homogeneous watersheds are identical except for a scaling factor. The flood frequency distribution is estimated at a given site by rescaling a dimensionless regional flood frequency distribution by the so-called index flood of the watershed, Q_{index}:

$$\widehat{Q}_i(T) = q_R(T) Q_{index}. \tag{1}$$

Where $\widehat{Q}_i(T)$ is the estimated T-year flood peak discharge for watershed i and $q_R(T)$ the dimensionless regional T-year flood also called growth factor, representative of a region. The regional growth factor is estimated from the normalized flood samples of a group of homogeneous gauged watersheds, $q_i(j)$:

$$q_i(j) = Q_i(j)/Q_{index}. \tag{2}$$

Where $Q_i(j)$ is the annual maximum flow for watershed i and year j. In this study, the scaling factor (index flood) will be defined by the mean annual maximum instantaneous flow discharge:

$$Q_{index} = E[Q_i]. \tag{3}$$

For gauged catchments, the sample mean annual maximum flow discharge is used:

$$\widehat{E[Q_i]} = \frac{1}{n}\sum_{j=1}^{n} Q_i(j) \tag{4}$$

For ungauged catchments, the mean annual maximum flow discharge is estimated by linear regression using physiographic and hydro-climatic catchment descriptors, x_k:

$$\widehat{E[Q_i]} = a_0 {x_1}^{a_1} {x_2}^{a_2} {x_3}^{a_3} ... {x_l}^{a_l}. \tag{5}$$

The model parameters a_k can be estimated by linear regression after logarithmic transformation or by non-linear regression (see for instance Grover *et al.*, 2002).

3.2 Flood probability distribution function and parameter estimation methods

The Generalized Extreme Value (GEV) distribution (Jenkinson, 1955) is adopted in this study, as in Crochet (2012a), for modeling the frequency distribution of both scaled and unscaled annual maximum flow series. The Cumulative Distribution Function (CDF) for the GEV distribution is:

$$G(q) = \text{Prob}(Q \leq q) = \begin{cases} \exp[-(1-\kappa(\frac{q-\varepsilon}{\alpha}))^{1/\kappa}] & \text{if } \kappa \neq 0 \\ \exp[-\exp(-\frac{q-\varepsilon}{\alpha})] & \text{if } \kappa = 0 \end{cases} \tag{6}$$

where Q is the random variable, q a possible value of Q, κ is the shape parameter, ε the location parameter and α the scale parameter. The GEV distribution combines into a single form the three types of limiting distributions for extreme values. Extreme value distribution Type 1 (κ=0), Type 2 (κ<0) and Type 3 (κ>0), respectively. The case with κ=0 corresponds to the Gumbel distribution. The p-th quantile which is the value q_p with cumulative probability p, ($G(q_p) = \text{Prob}(Q \leq q_p) = p$), is estimated as follows:

$$\widehat{q_p} = \begin{cases} \varepsilon + \frac{\alpha}{\kappa}(1-[-\ln(p)]^{\kappa}) & \text{if } \kappa \neq 0 \\ \varepsilon - \alpha\ln(-\ln(p)) & \text{if } \kappa = 0 \end{cases} \tag{7}$$

The p-th quantile is associated to the return period $T = 1/(1-p)$ and can also be written as follows:

$$\widehat{q}(T) = \begin{cases} \varepsilon + \frac{\alpha}{\kappa}(1-[-\ln(1-1/T)]^{\kappa}) & \text{if } \kappa \neq 0 \\ \varepsilon - \alpha\ln(-\ln(1-1/T)) & \text{if } \kappa = 0 \end{cases} \tag{8}$$

Several approaches are available for estimating the parameters of the GEV distribution, such as the Maximum Likelihood (ML) and the Probability Weigthed Moments (PWM) or the equivalent L-moments (LMOM). The PWM method will be adopted here as it is supposed to be more robust than the ML method for small samples (Hosking *et al.*, 1985a), which is the case here.

3.3 Regional growth factor

The regional growth factor describes the dimensionless regional flood frequency distribution, $q_R(T)$. It is estimated in this study with the regionalization algorithm proposed by Hosking *et al.* (1985b). First, the GEV distribution of the annual maximum flow is estimated at each gauged site, i, belonging to a homogeneous region of N sites, by estimating the PWMs, $\hat{\beta}_r{}^i$,

(r=0,1,2), as defined in Hosking *et al.* (1985a). These PWMs are then scaled by $\hat{\beta}_0{}^i$, the sample mean, to obtain for each site the quantities $\hat{t}_1{}^i = \hat{\beta}_1{}^i/\hat{\beta}_0{}^i$ and $\hat{t}_2{}^i = \hat{\beta}_2{}^i/\hat{\beta}_0{}^i$. Then, the regional estimators $\hat{t}_j{}^R = \sum_{i=1}^N \hat{t}_j{}^i n_i / \sum_{i=1}^N n_i$, ($j$=1,2), are calculated, where n_i represents the sample size at site i. Finally, the regional PWMs are derived by setting $\hat{\beta}_0{}^R = 1$, $\hat{\beta}_1{}^R = \hat{t}_1{}^R$ and $\hat{\beta}_2{}^R = \hat{t}_2{}^R$ and the parameters κ_R, ε_R and α_R of the regional GEV distribution, or regional growth curve, are estimated. Finally, the estimated flood quantile $\widehat{Q}_i(T)$ at a given site i, is calculated with Eq. (1). The index flood Q_{index} is calculated either by Eq. (4) or Eq. (5) and $\hat{q}_R(T)$ given by:

$$\widehat{q}_R(T) = \begin{cases} \varepsilon_R + \frac{\alpha_R}{\kappa_R}(1 - [-\ln(1-1/T)]^{\kappa_R}) & \text{if } \kappa_R \neq 0 \\ \varepsilon_R - \alpha_R \ln(-\ln(1-1/T)) & \text{if } \kappa_R = 0 \end{cases} \tag{9}$$

3.4 Confidence intervals for quantiles

The uncertainty associated to the quantile $\widehat{Q}_i(T)$ is usually expressed in form of a confidence interval. The upper and lower bounds of the $100(1-\theta)\%$ confidence interval of $\widehat{Q}_i(T)$ are given by:

$$\widehat{Q}_i(T) \pm z_{1-\theta/2}\sqrt{\mathrm{Var}\{\widehat{Q}_i(T)\}} \tag{10}$$

where $z_{1-\theta/2}$ is the upper point of the standard normal distribution exceeded with probability $\theta/2$ and the variance of the T-year flood at site i is estimated by:

$$\mathrm{Var}\{\widehat{Q}_i(T)\} = \mathrm{Var}\{\widehat{q}_R(T)\}\widehat{E[Q_i]}^2 + \mathrm{Var}\{\widehat{E[Q_i]}\}E[\widehat{q}_R(T)]^2 \tag{11}$$

With $E[\widehat{q}_R(T)] = \widehat{q}_R(T)$. The asymptotic variance of the three-parameter GEV/PWM p-th quantile (here the regional growth factor $q_R(T)$), $\mathrm{Var}\{\widehat{q}_R(T)\}$ can be found in Lu *and* Stedinger (1992) and is also given in Crochet (2012a). The elements of the asymptotic covariance matrix for the estimators ε_R, α_R and κ_R can be found in Hosking *et al.* (1985a). The formulas for calculating the variance of the mean annual maximum flow, $\mathrm{Var}\{\widehat{E[Q_i]}\}$, when $\widehat{E[Q_i]}$ is estimated either with Eq. (4) or Eq. (5) can be found in books on statistical analysis and regression analysis.

3.5 Delineation of homogeneous regions

In Crochet (2012a), two groups of watersheds were defined according to their geographic proximity. The first group was located in the Tröllaskagi region and surroundings (vhm 10, vhm 45, vhm 51, vhm 92, vhm 200) and the second group was located in the West-fjords and surroundings (vhm 19, vhm 38, vhm 198, vhm 204, vhm 12). Two additional techniques are now considered for the objective delineation of homogeneous regions (DHR) and compared to the geographic delineation used as benchmark. These two techniques were recently used in Malekinezhad *et al.* (2011b) for instance.

3.5.1 Region of influence

The region of influence (ROI) technique was developed by Burn (1990a, 1990b). With this method, a potentially unique "region", or region of influence, is defined for each gauging station.

The advantage of this method is that there is no need to define geographic boundaries between regions and each site can have its own region, made of all the watersheds considered sufficiently similar to produce a similar hydrologic response with respect to extreme flow. First, a set of p attributes describing each watershed has to be defined. Then a distance metric is selected to measure the similarity/dissimilarity of the watershed to every other watershed according to these attributes. The following distance metric, D_{ki}, measuring the Euclidian distance between watershed k and watershed i with respect to all p attributes, is used:

$$D_{ki} = \sqrt{\sum_{j=1}^{p} \left(\frac{C_j^k - C_j^i}{S_{C_j}} \right)^2} \tag{12}$$

Where C_j^k is the value of $j-th$ attribute at site k, C_j^i is the value of $j-th$ attribute at site i and S_{C_j} is the sample standard-deviation of $j-th$ attribute across all sites. The standardization by S_{C_j} eliminates the units from each attribute and reduces any differences in the range of values among the attributes (Burn, 1990b).

The distance metric D_{ki} is then sorted and only the N_k sites i for which $D_{ki} < \theta_k$ are selected. The threshold value θ_k is defined as follows:

$$\theta_k = \begin{cases} \theta_l & \text{if } N_k \geq N_0 \\ \theta_l + (\theta_u - \theta_l)\frac{N_0 - N_k}{N_0} & \text{if } N_k < N_0 \end{cases} \tag{13}$$

Where θ_l and θ_u are the desired lower and upper threshold values for D_{ki}, respectively and N_0 is the desired minimum number of stations to be included in the ROI. The threshold θ_k is raised until the target number of stations, N_0, is reached. By increasing the threshold, more stations are included at the expense of homogeneity but a sufficient number of stations is required to derive the index flood through linear regression and allow the transfer of information to the ungauged site k, so a compromise must be found. As the number of watersheds analyzed was relatively small, N_0 was set to a minimum of four watersheds in this study and the 40% and 80% percentile distances (D_{ki}) were used as a starting point for defining θ_l and θ_u.

The sorted distance metric D_{ki} ranks the proximity of each selected watershed i to the target watershed k. A weight is then defined to reflect the relative importance to be given to each watershed i for the estimation of the extreme flow statistics at site k:

$$WF_{ki} = 1 - \left(\frac{D_{ki}}{THL} \right)^n \tag{14}$$

where WF_{ki} is the weight given to site i in the ROI for site k, n is a positive constant and THL is a parameter. The values of THL was set to the 85% percentile of D_{ki} and n was set to 2.5, as in Burn (1990b). These weights are then included in the calculation of the regional PWMs for the estimation of the regional growth curve (see Section 3.3) as:

$$\hat{t}_j^{\,R} = \sum_{i=1}^{N_k} \hat{t}_j^{\,i} n_i WF_{ki} / \sum_{i=1}^{N_i} n_i WF_{ki}, (j = 1, 2) \tag{15}$$

3.5.2 Hierarchical clustering

Cluster analysis is a well known method used in a variety of research problems to divide datasets into mutually exclusive and jointly exhaustive groups. Two types of hierarchical clustering technique exist, agglomerative and divisive. The agglomerative techniques start by defining one cluster per site and then iteratively merge the two nearest clusters according to a merging cost until only one cluster with all sites remains. Divisive clustering techniques start by forming one large cluster with all sites and split them iteratively according to a dissimilarity measure until each site forms its own cluster. The different clustering algorithms will give different results on the same data. The Ward's method, which is an agglomerative hierarchical clustering technique was used in this study. The same distance metric used in the ROI method (Eq. 12) was used here as dissimilarity measure. Two clusters were extracted with at least four stations in each so as to ensure that the index flood could be calculated by simple linear regression.

3.6 Test of homogeneity for a region

Once an homogeneous group of watersheds has been preliminary delineated according to the selected watershed attributes, the degree of homogeneity of the candidate group with respect to extreme flow statistics remains to be tested. The H-statistics, proposed by Hosking *and* Wallis (1993), based on L-moment ratios, is used here as guideline. Recent examples of application of this test in regional flood frequency analysis can be found in Jingyi *and* Hall (2004), Das *and* Cunnane (2011) and Malekinezhad *et al.* (2011a and 2011b) for instance. The idea is to measure the sample L-moment ratios and compare it to the variation that would be expected in a homogeneous region.

First the L-moment ratios of each site i are calculated. The first four L-moments are derived from the PWMs, $\hat{\beta}_r{}^i$ (see Section 3.3) as follows:

$$\begin{cases} \hat{\lambda}_1 = \hat{\beta}_0 \\ \hat{\lambda}_2 = 2\hat{\beta}_1 - \hat{\beta}_0 \\ \hat{\lambda}_3 = 6\hat{\beta}_2 - 6\hat{\beta}_1 + \hat{\beta}_0 \\ \hat{\lambda}_4 = 20\hat{\beta}_3 - 30\hat{\beta}_2 + 12\hat{\beta}_1 - \hat{\beta}_0 \end{cases} \tag{16}$$

and the L-moment ratios are defined as:

$$\begin{cases} t^i = \hat{\lambda}_2/\hat{\lambda}_1 \\ t_3{}^i = \hat{\lambda}_3/\hat{\lambda}_2 \\ t_4{}^i = \hat{\lambda}_4/\hat{\lambda}_2 \end{cases} \tag{17}$$

where t^i is the L-CV, $t_3{}^i$ is the L-skewness and $t_4{}^i$ is the L-kurtosis at site i. Then, the regional averaged L-moment ratios are estimated as follows:

$$\begin{cases} \hat{t}^R = \sum_{i=1}^{N_k} n_i t^i / \sum_{i=1}^{N_k} n_i \\ \hat{t}_3{}^R = \sum_{i=1}^{N_k} n_i t_3{}^i / \sum_{i=1}^{N_k} n_i \\ \hat{t}_4{}^R = \sum_{i=1}^{N_k} n_i t_4{}^i / \sum_{i=1}^{N_k} n_i \end{cases} \tag{18}$$

A four-parameter Kappa distribution is fitted to the regional averaged L-moment ratios which is then used to simulate a series of 500 equivalent homogeneous regions (of N_k sites) whose L-statistics variability is then compared to the variability of the L-statistics of the actual region. Two homogeneity measures (H-statistics) have been employed to test the variability of the L-statistics: H_1 for L-CV and H_2 for the combination of L-CV and L-skewness.

The H_1-statistics is defined as follows:

$$H_1 = \frac{V_{1obs} - \mu_{V_1}}{\sigma_{V_1}} \tag{19}$$

where

$$V_1 = \left\{ \frac{\sum_{i=1}^{N_k} n_i \left(t^i - \hat{t}^R \right)^2}{\sum_{i=1}^{N_k} n_i} \right\}^{1/2} \tag{20}$$

and μ_{V_1} and σ_{V_1} are the mean and standard-deviation of the simulated values of V_1 and V_{1obs} is the value of V_1 derived from the experimental data of the region under study.

The H_2-statistics is defined as follows:

$$H_2 = \frac{V_{2obs} - \mu_{V_2}}{\sigma_{V_2}} \tag{21}$$

where

$$V_2 = \frac{\sum_{i=1}^{N_k} n_i \left\{ \left(t^i - \hat{t}^R \right)^2 + \left(\hat{t}_3{}^i - \hat{t}_3{}^R \right)^2 \right\}^{1/2}}{\sum_{i=1}^{N_k} n_i} \tag{22}$$

and μ_{V_2} and σ_{V_2} are the mean and standard-deviation of the simulated values of V_2 and V_{2obs} is the value of V_2 derived from the experimental data of the region under study.

According to the test, a region is acceptably homogeneous if $H < 1$, possibly heterogeneous if $1 \leq H < 2$ and definitely heterogeneous when $H \geq 2$. The H_1 statistics is usually considered more powerful than H_2.

4 Results

The two delineation methods presented above were applied to identify homogeneous regions and then to calculate the regional growth curves ($q_R(T)$) and index flood (Q_{index}). A large number of watershed attributes and combination of attributes were defined and tested for the calculation of the distance metric D_{ki}. These attributes include physiographic attributes such as drainage area (A), mean catchment altitude (Z), catchment perimeter (L); climatic attributes such as mean annual basin-averaged precipitation (P) for the period 1971–2000; and hydrologic attributes such as basin-averaged saturated hydraulic conductivity (K_{sat}), simulated daily water available for runoff (WQ_R) and variables derived from WQ_R. The simulated water available for runoff, WQ_R, was calculated for each watershed as the sum of rain and snowmelt, derived from gridded daily precipitation data (Crochet *et al.*, 2007), air temperature data (Crochet *and* Jóhannesson, 2011) and a simple degree day melt model (Crochet, 2012b). It is expected to give a more elaborate information about the hydrological characteristics of the watersheds than just precipitation, and also to provide a simple description of the hydrologic regime for watersheds where no streamflow data are available. It was not however the intent of this work to develop a full hydrologic model. Annual maximum WQ_R values were extracted (WQ_Rmax) and quantiles estimated for various return periods T, using the GEV distribution ($WQ_Rmax(T)$). Then, WQ_R was smoothed using a 5-day running mean (WQ_R5d) and a mean daily hydrograph calculated for the period 1958–2006 ($WQ_R5d(58-06)$), from which i) the annual maximum value was extracted: $Max(WQ_R5d(58-06))$, ii) its date of occurrence: $t_{WQ_R5d(58-06)}$, and iii) the number of days with $WQ_R5d(58-06)$ above a threshold defined as 2/3 of $Max(WQ_R5d(58-06))$: $D_{WQ_R5d(58-06)}$. The results obtained for the homogeneous regions delineated with the following two sets of attributes are presented:

Set_1: Average watershed elevation (Z); average saturated hydraulic conductivity (K_{sat}); ratio between basin perimeter (L) and perimeter of circle of area equal to catchment area (L_C); mean annual basin-averaged precipitation (P); simulated daily water available for runoff, averaged over 1958–2006, and normalized by catchment area: $WQ_R5d(58-06)/A$.

Set_2: Natural logarithm of drainage area ($log(A)$); average watershed elevation (Z); average saturated hydraulic conductivity (K_{sat}); mean annual basin-averaged precipitation (P); and hydrologic characteristics derived from the simulated water available for runoff : $Max(WQ_R5d(58-06))$; $t_{WQ_R5d(58-06)}$; $D_{WQ_R5d(58-06)}$; water available for runoff growth curve for return periods T=10, 50 and 100 years: $WQ_Rmax(T)/E[WQ_Rmax]$.

4.1 Regional growth curves

4.1.1 Geographic delineation

Figure 2 presents the growth curves for each catchment and the estimated regional growth curves corresponding to the two geographic regions, respectively, with the estimated 95% confidence interval. The H-statistics are also given. One can see that according to the H_1-statistics, Region 2 is definitely homogeneous while Region 1 did not pass the test and was flagged as heterogeneous, but according to the H_2-statistics, it was homogeneous. Table 2 presents the H_1-statistics and H_2-statistics obtained for each region without the target station, i.e. by eliminating one station at the time, to be compared to H_1-statistics and H_2-statistics given in Figure 2, calculated with all stations of each region. The different flood series do not always correspond to the same period for the different watersheds and some heterogeneity could result from climate variability. Outliers could also account for some of the discrepancies, especially the largest values, because of uncertainties in the rating curves used to convert extreme water-levels into extreme discharge.

4.1.2 Hierarchical clustering

Figure 3 presents the dendrograms showing the hierarchy among watersheds, according to the Wards's clustering approach. The first set of attributes, set_1, delineated the same two regions than the geographic delineation method described above and results were therefore identical. The second set of attributes, set_2, delineated two clusters of watersheds different from those obtained with set_1, mixing watersheds from the two geographic regions. Cluster 1 is made of vhm 10, vhm 45, vhm 12, vhm 38, vhm 198. Cluster 2 is made of vhm 51, vhm 92, vhm 200, vhm 19, vhm 204. Figure 4 presents the growth curves for each catchment and the estimated regional growth curves for each cluster, delineated with the second set of attributes, set_2. Figures 5 and 6 present all the estimated regional growth curves calculated without the target watersheds. Table 3 presents the H_1-statistics and H_2-statistics obtained for each cluster, without the target station, i.e. by eliminating one station at the time, to be compared to H_1-statistics and H_2-statistics given in Figure 3 which were obtained with all stations of each cluster. According to both H_1-statistics and H_2-statistics (Fig. 3), both clusters delineated with second set of attributes, set_2, are homogeneous, but when the target station is not used, some clusters are no longer considered homogeneous.

4.1.3 Region of influence

With this method, a ROI is associated to each watershed. Table 4 presents the H_1-statistics and H_2-statistics obtained for each ROI, delineated with the two sets of attributes, set_1 or set_2, and calculated with all ROI stations, and then without the target station. The corresponding regional and at-site growth curves, obtained with the first set of attributes set_1 are presented in Appendix 1. The H_1-statistics indicate that some of the identified ROIs did not pass the homogeneity test according to the H_1-statistics, such as the ROI of vhm 10, vhm 12, vhm 38, vhm 45, vhm 92, vhm 198 and vhm 200, delineated with set_1 and the ROI of vhm 12, vhm 51 and vhm 204 delineated with set_2, but most of them passed the homogeneity test according to the H_2-statistics. It is also interesting to note that for a given set of attributes, ROI and the cluster analysis did not always agree and delineated different regions. Reducing the number of watersheds belonging to the ROI, in order to obtain a more reasonable H_1-statistics, will be problematic for the estimation of the index flood.

4.2 Index flood parameter

The index flood parameter, namely the mean annual maximum instantaneous flow, $E[Q_i]$ (Eq. (3)), was estimated by the sample mean (Eq. (4)), for gauged catchments, and modeled with Eq. (5), considering the following watershed physiographic attributes: drainage area (A), mean catchment altitude (Z), catchment perimeter (L), and the following hydro-climatic attributes: mean annual basin-averaged precipitation for the standard period 1971–2000 (P) and mean annual maximum water available for runoff ($Q_S = E[WQ_Rmax]$). The limited number of catchments under study restricts the number of variables that can be used in the multiple linear regression model. It was thus decided to define one single explanatory variable by combining several of these attributes together. The six following models have been tested and evaluated using ordinary least squares (OLS) after logarithmic transformation:

$$\widehat{E[Q_i]} = aA^b \tag{23}$$

$$\widehat{E[Q_i]} = a(AP)^b \tag{24}$$

$$\widehat{E[Q_i]} = a(AP/Z)^b \tag{25}$$

$$\widehat{E[Q_i]} = a(Q_s/z)^b \tag{26}$$

$$\widehat{E[Q_i]} = a(Q_s)^b \tag{27}$$

$$\widehat{E[Q_i]} = a(A/L)^b \tag{28}$$

Table 2. Geographic delineation: H-statistics for each region without target stations.

Region 1 without :	vhm 10	vhm 51	vhm 92	vhm 200	vhm 45
H_1	2.1	1.2	2.8	2.3	2.4
H_2	-0.624	-0.47	-0.2	-0.44	-0.8
Region 2 without :	vhm 12	vhm 19	vhm 38	vhm 198	vhm 204
H_1	-0.751	-0.08	0.5	-0.013	0.0
H_2	-0.61	-0.78	-0.63	-0.09	-0.04

Table 3. Cluster delineation using second set of attributes (set_2): H-statistics without target stations.

Cluster 1 without :	vhm 10	vhm 45	vhm 12	vhm 38	vhm 198
H_1	0.66	0.02	-0.19	1.2	0.66
H_2	0.29	-0.45	-0.48	-0.51	0.06
Cluster 2 without :	vhm 51	vhm 92	vhm 200	vhm 19	vhm 204
H_1	0.45	2.17	1.6	1.9	2.8
H_2	-1	-0.93	-1.07	-1.06	-0.5

Table 4. ROI delineation: H-statistics with and without target stations.

	vhm 10	vhm 51	vhm 92	vhm 200	vhm 45
Ref H_1 from set_1	2.19	1.76	2.5	2.2	2.3
H_1 from set_1	2.37	0.17	2.8	2.5	2.3
Ref H_2 from set_1	-0.25	-0.6	-0.5	-0.12	-0.23
H_2 from set_1	0.23	-0.8	-0.24	0.1	-0.27
Ref H_1 from set_12	0.6	2.6	1.8	1.9	0.54
H_1 from set_2	0.7	0.65	2.25	1.7	0.06
Ref H_2 from set_2	-0.3	-0.6	-1.1	-1.2	-0.44
H_2 from set_2	0.3	-1.1	-0.85	-1.08	-0.46
	vhm 12	vhm 19	vhm 38	vhm 198	vhm 204
Ref H_1 from set_1	2.6	-0.13	2	2.3	-0.18
H_1 from set_1	1.8	-0.05	3.1	2.8	-0.03
Ref H_2 from set_1	-0.1	-0.51	-0.02	-0.05	-0.5
H_2 from set_1	-0.41	-0.66	-0.27	0.46	-0.02
Ref H_1 from set_12	2.8	-0.06	-0.06	-0.09	2.6
H_1 from set_2	1.74	-0.11	0.3	0.02	3.4
Ref H_2 from set_2	0.013	-0.44	-0.7	-0.81	-0.79
H_2 from set_2	-0.47	-0.65	-1.11	-0.44	-0.14

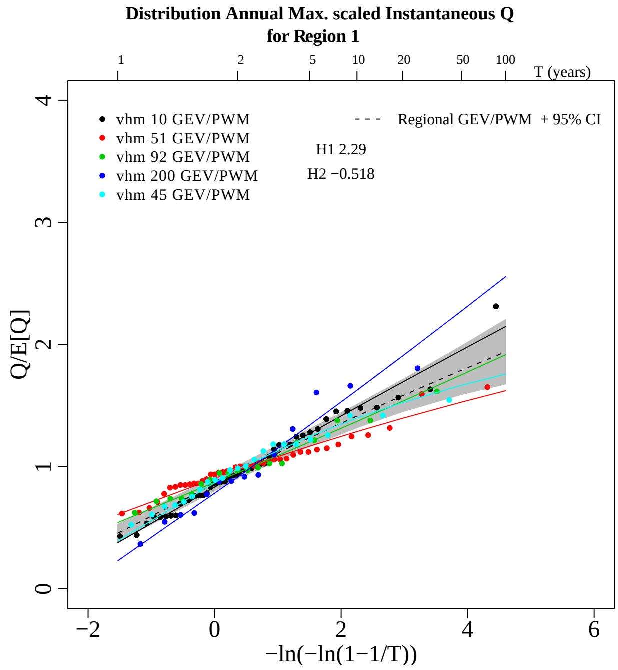

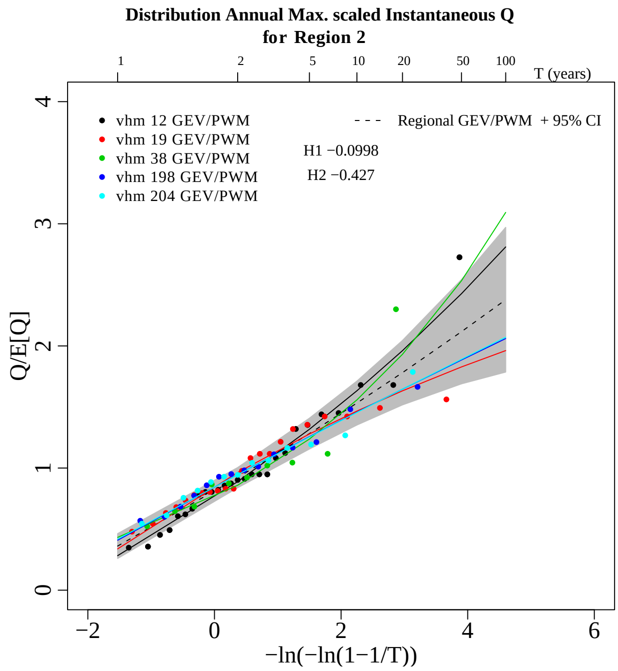

Figure 2. Growth curves for each catchment and regional growth curves for the two geographic regions: Region 1 (top) and Region 2 (bottom). The grey shaded region corresponds to the 95% confidence interval of the regional growth curve.

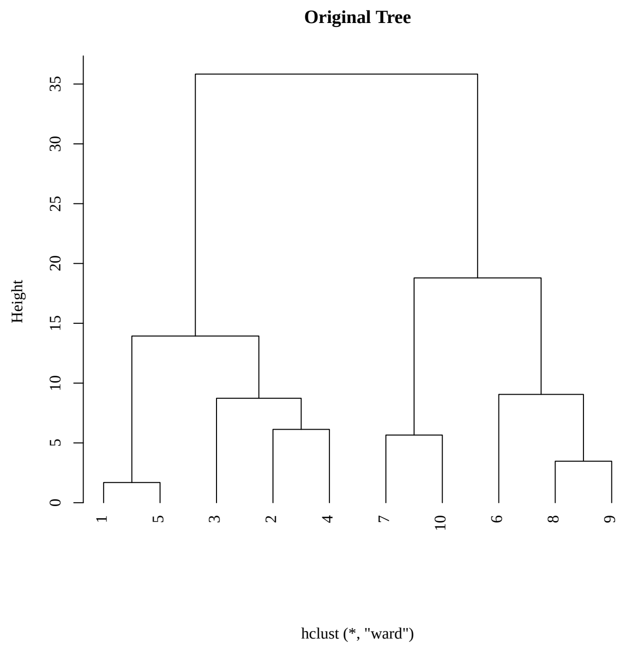

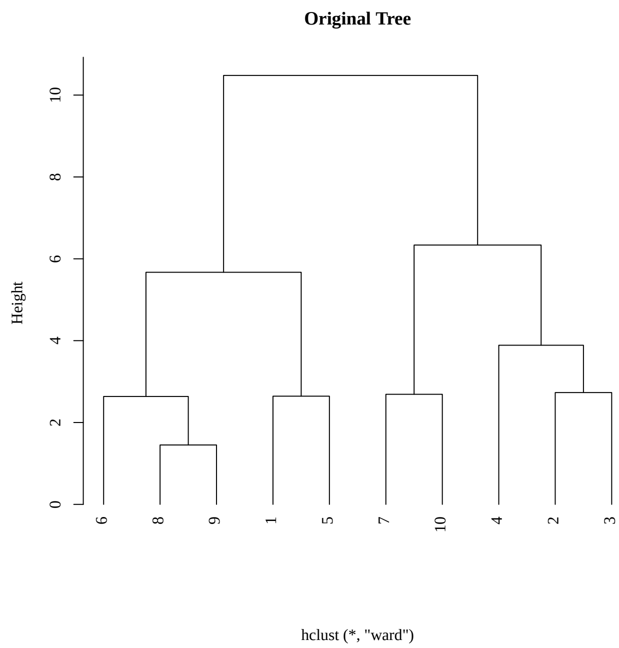

Figure 3. Cluster analysis using the Ward's method with first set of attributes, set_1, (top), and second set of attributes, set_2, (bottom). The number on the x-axis refers to the catchment rank as listed in Table 1.

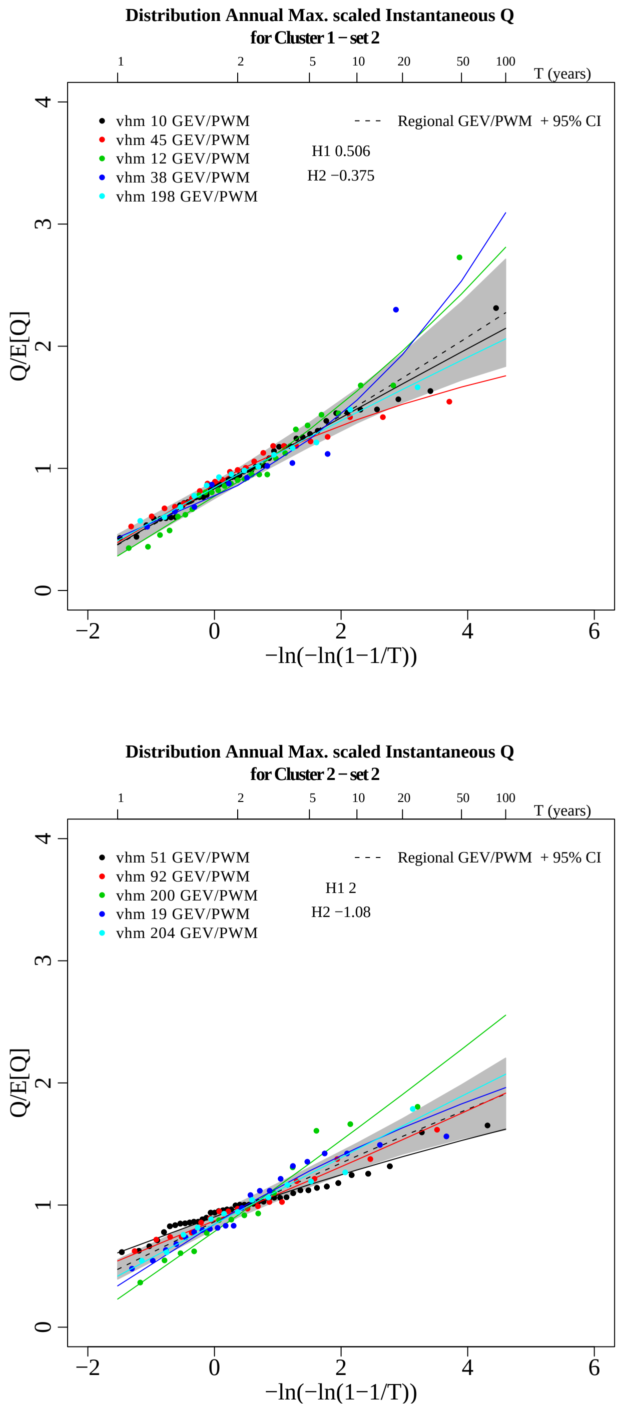

Figure 4. Growth curves for each catchment and regional growth curves for the two regions delineated by cluster analysis using the second set of attributes, set$_2$: Cluster 1 (top) and Cluster 2 (bottom). The grey shaded region corresponds to the 95% confidence interval of the regional growth curve.

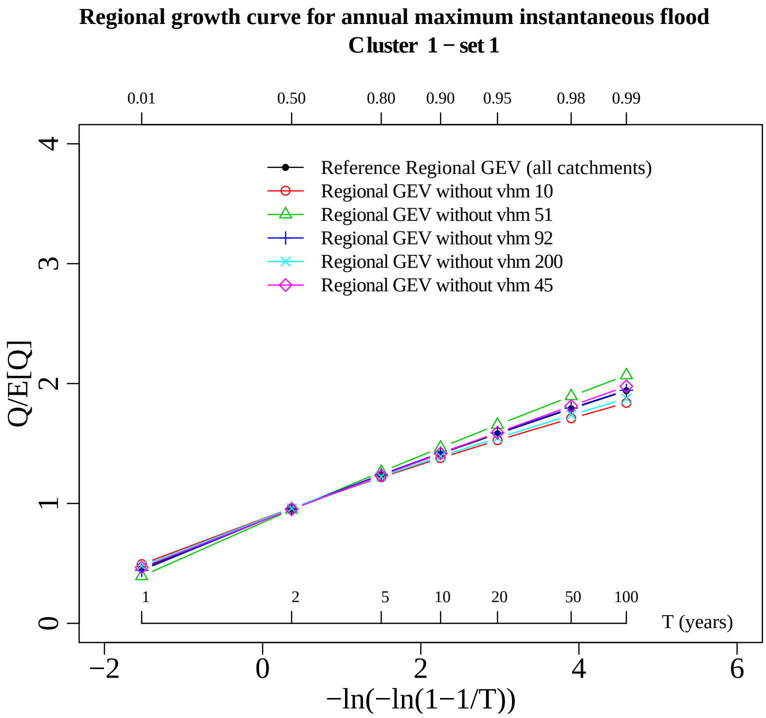

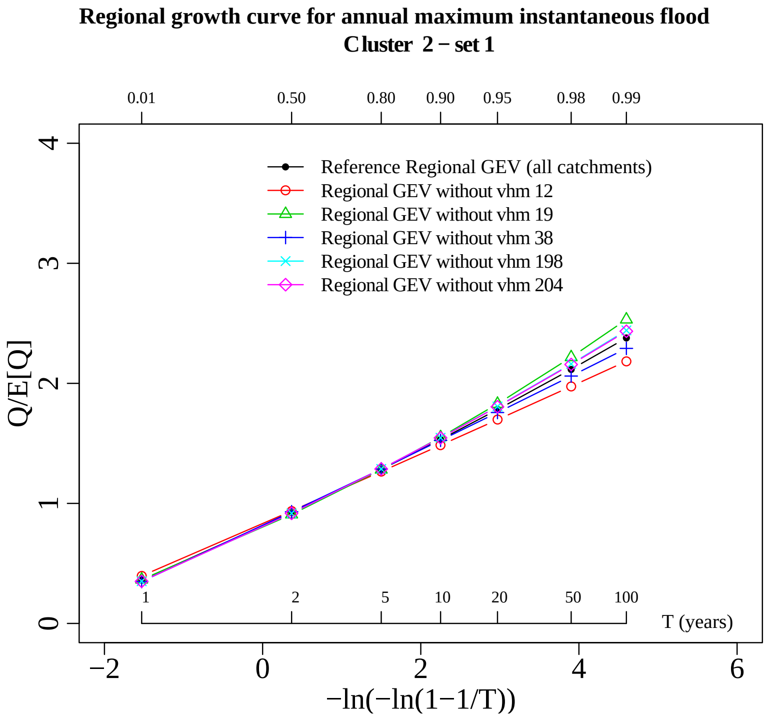

Figure 5. Cluster delineation method using first set of attributes, set_1 (equivalent to geographic delineation method): Regional growth curves calculated without the target watershed for Cluster 1 (top) and Cluster 2 (bottom).

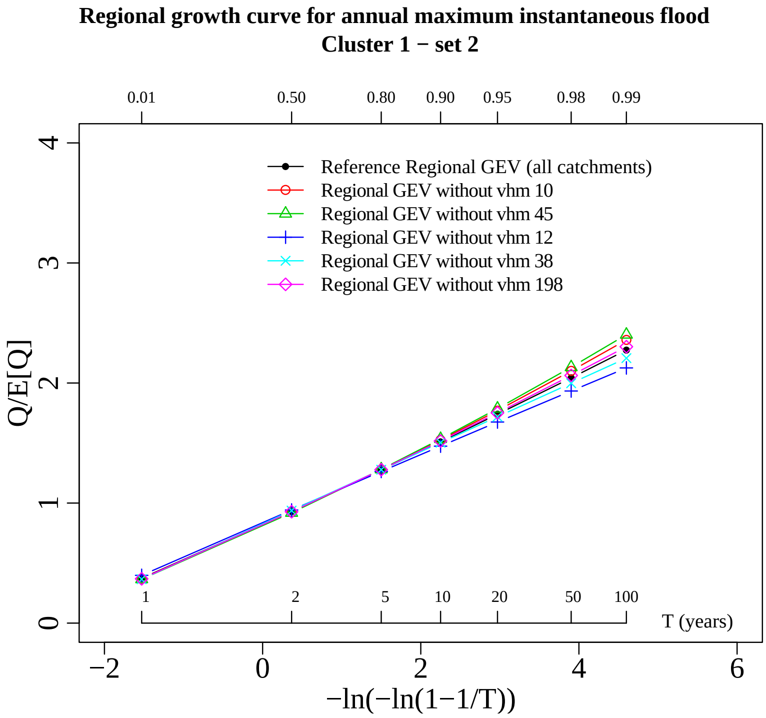

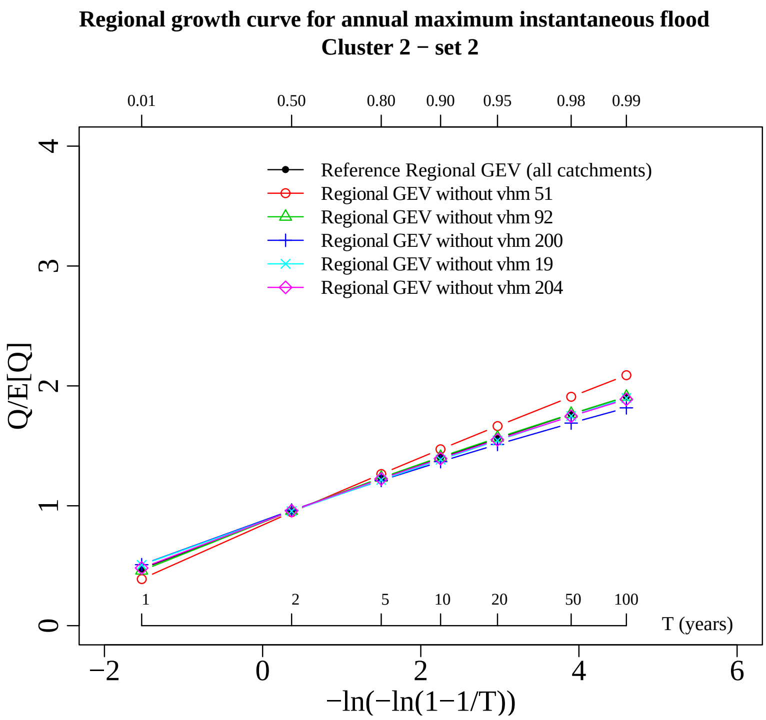

Figure 6. Cluster delineation method using second set of attributes, set$_2$: Regional growth curves calculated without the target watershed for cluster 1 (top) and cluster 2 (bottom).

4.3 Flood frequency distribution for ungauged catchments

In order to evaluate the methodology for ungauged catchments and simulate their flood frequency distribution which will then be used to derive the T-year flood peak discharge, the same cross-validation methodology as employed in Crochet (2012a) was used here. Each of the 10 watersheds was in turn defined as the target watershed, assumed "ungauged", and its flood data set used as reference only in the validation of the methodology but neither in the calculation of the regional growth curve nor in the calibration of the linear regression models used to estimate the index flood. In practice, for a group of N_k watersheds, $N_k - 1$ watersheds were used to estimate the regional growth curve and the index flood, to be applied in the calculation of the T-year flood peak discharge at the N_k^{th} watershed, called the target watershed. Following this methodology, the flood frequency distribution of each river basin was obtained by combining a method for delineating the homogeneous region (DHR) and a regional estimation method (REM) (Eq. 1), which in the present context constitutes a regional model, according to the terminology defined by GREHYS (1996b). The regional estimation method includes in this case the estimation of the growth curves (Eq. 9) and the index flood (Eqs. 23–28). Three different delineation methods (DHR) were used, two of them with two different sets of attributes each, and six regional estimation methods (REM) were used to calculate the index flood and derive the flood frequency distribution. This gives a total of 30 (5x6) different regional models, $M_R[i,j] = DHR[i]xREM[j]$ where i and j correspond to particular methods:

- $DHR[1]$: Geographic delineation
- $DHR[2]$: Ward's hierarchical clustering using first set of attributes, "set_1"
- $DHR[3]$: ROI using first set of attributes, "set_1"
- $DHR[4]$: Ward's hierarchical clustering using second set of attributes, "set_2"
- $DHR[5]$: ROI using second set of attributes, "set_2"

- $REM[1:6]$: Index flood estimation calculated with Eqs. 23 to 28

Regional models $M_R[1,j]$ and $M_R[2,j]$ are identical, as the two delineated regions were the same. The quality of the estimated index flood was evaluated for each regional model over all (N) watersheds, by calculating the RMSE:

$$RMSE[i,j] = \sqrt{\frac{1}{N}\sum_{k=1}^{N}\left(E[Q_k] - \widehat{E[Q_k]}\right)^2}, \tag{29}$$

Figures 7 to 10 present the estimated vs. observed index flood for each watershed and their respective RMSE. The best results are usually obtained when both physiographic and hydro-climatic descriptors are used. Usually, the best index flood estimation model will be different for the different watersheds, but one has to be selected, giving the overall best results. The lowest $RMSE$ score over all watersheds was obtained with $REM[2]$ for $DHR[1]$ and $DHR[2]$, with $REM[4]$ for $DHR[3]$, with $REM[2]$ for $DHR[4]$ and with $REM[3]$ for $DHR[5]$. The best overall estimation was obtained with $M_R[5,3]$ ($DHR[5]xREM[3]$).

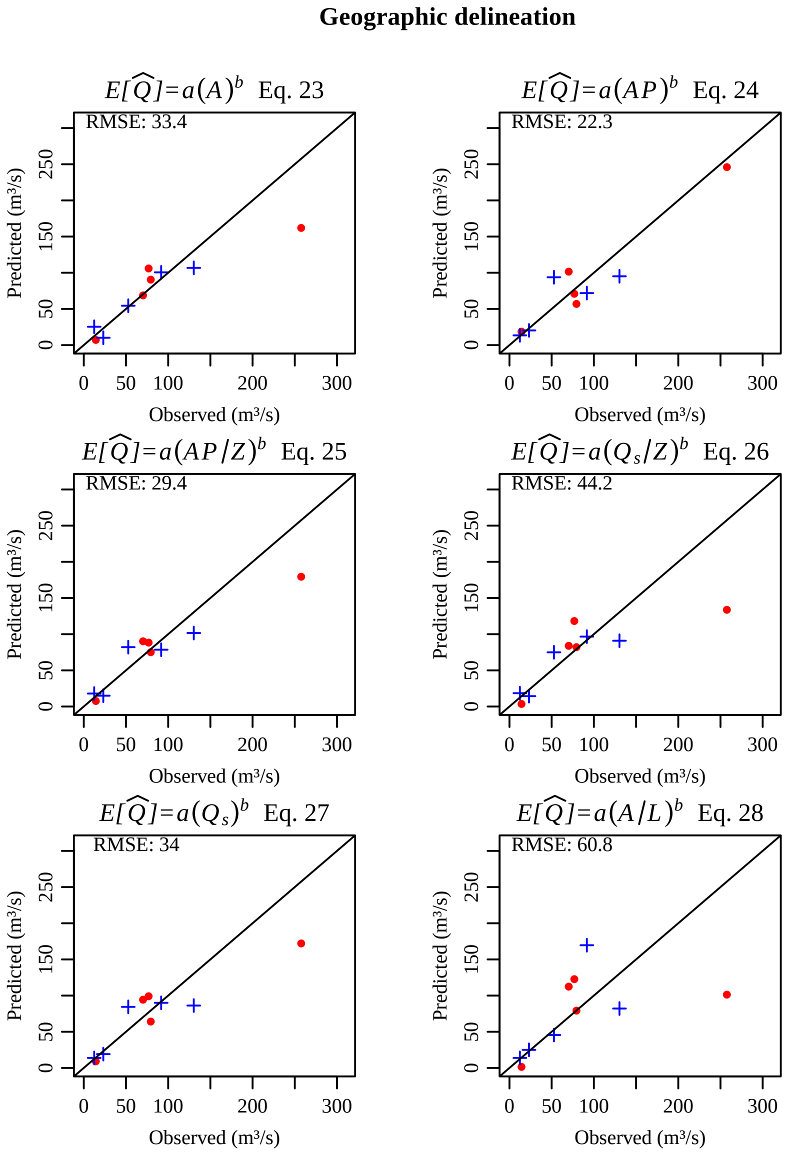

Figure 7. Index flood estimation at "ungauged" catchments using the geographic delineation method. Cross-validation.

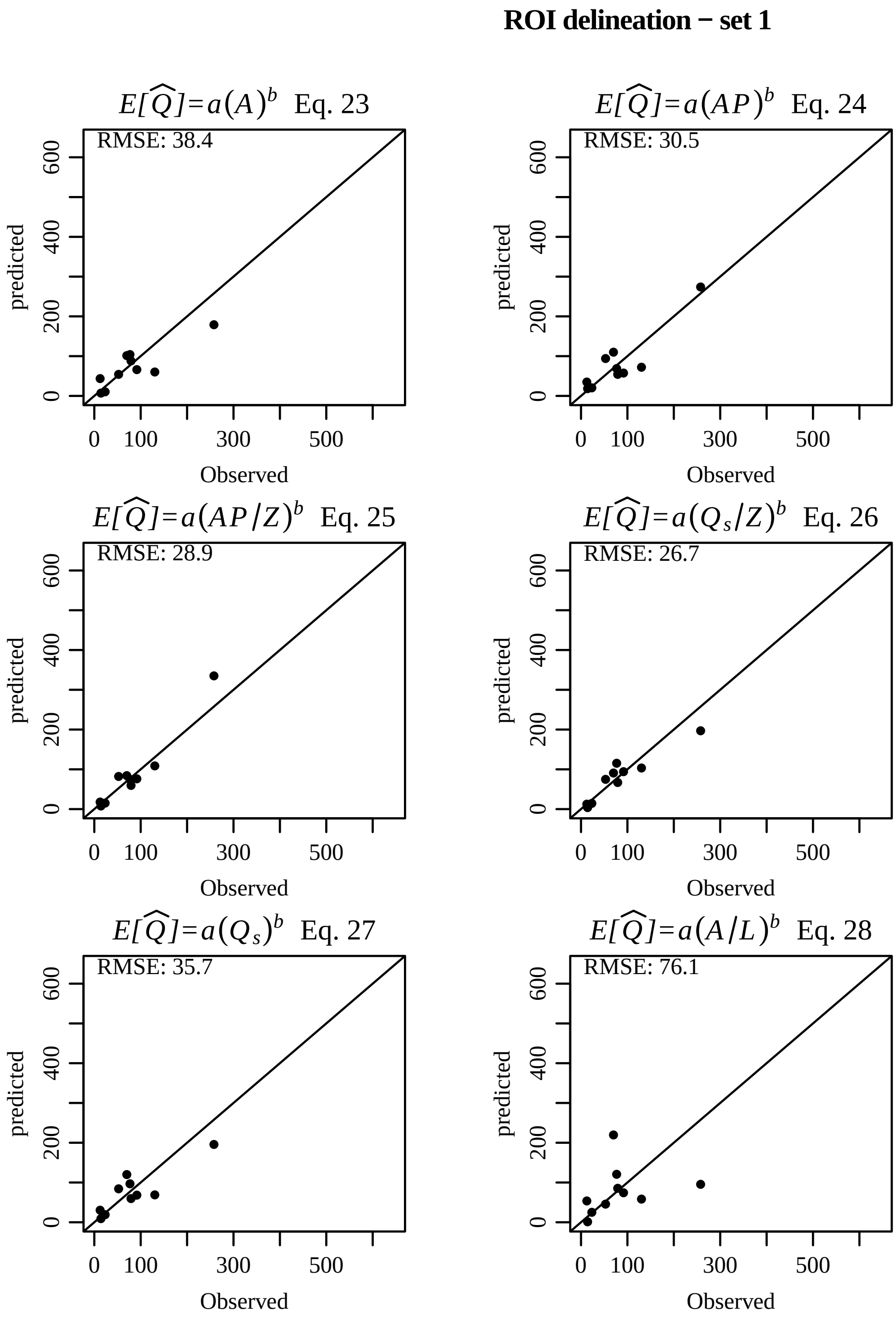

Figure 8. Index flood estimation at "ungauged" catchments using the ROI delineation method with first set of attributes (set_1). Cross-validation.

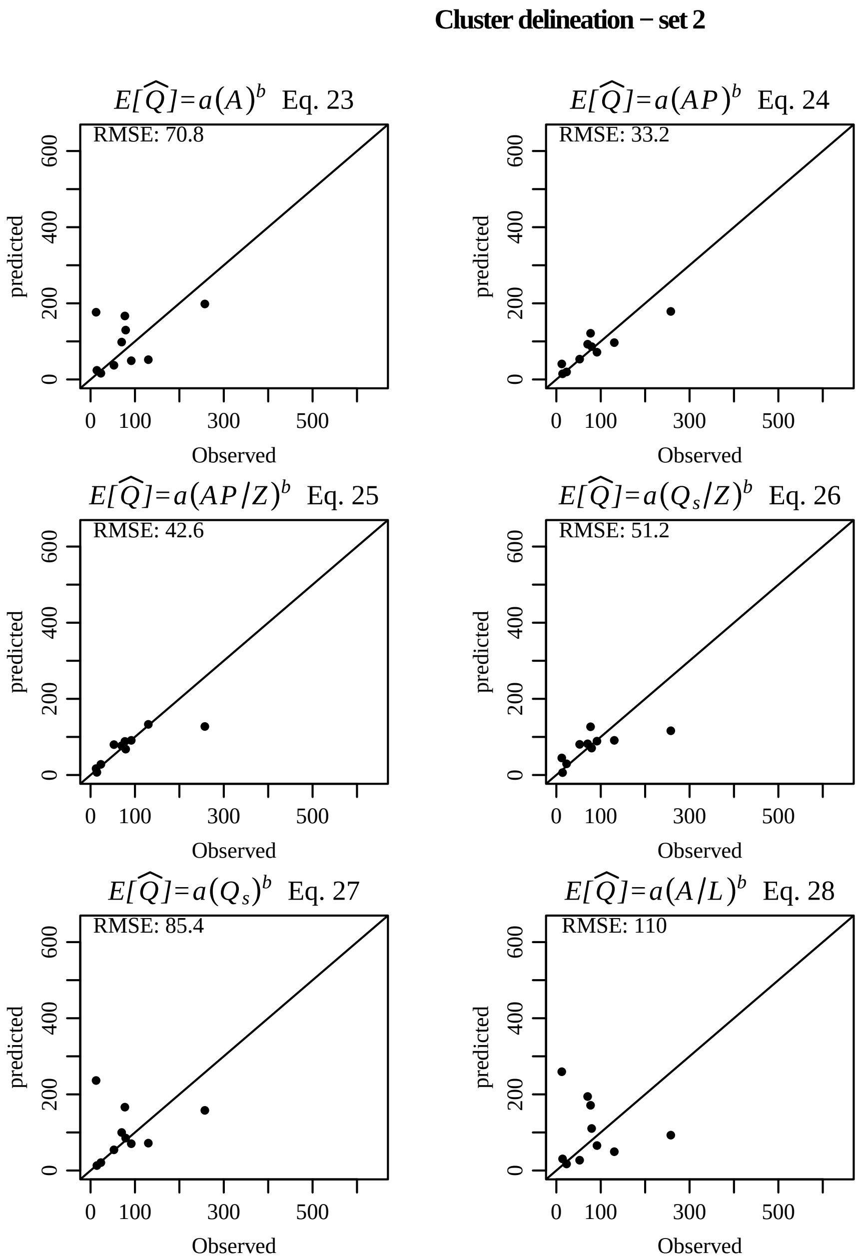

Figure 9. Index flood estimation at "ungauged" catchments using the clustering delineation method with second set of attributes (set_2). Cross-validation.

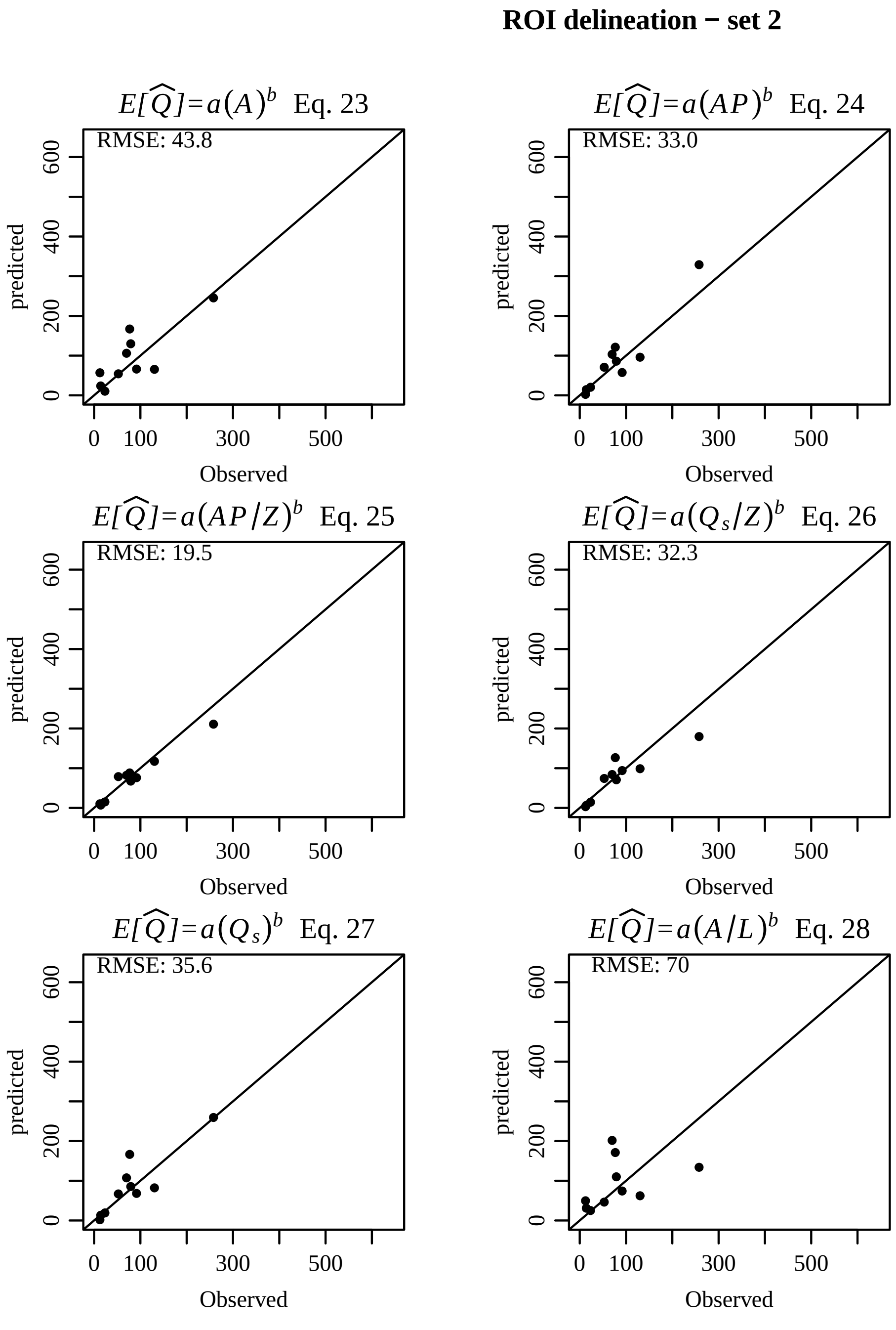

Figure 10. Index flood estimation at "ungauged" catchments using the ROI delineation method with second set of attributes (set_2). Cross-validation.

The quality of the estimated flood frequency distributions was evaluated for each watershed, by calculating the following statistics on the flood quantiles:

$$RMSE_{Q_T}[i,j,k] = \sqrt{\frac{1}{L}\sum_{l=1}^{L}\left(Q_k(T_l) - \widehat{Q_k}(T_l)\right)^2}, \tag{30}$$

$$TS_1[i,j] = \frac{1}{N}\sum_{k=1}^{N} RMSE_{Q_T}[i,j,k] \tag{31}$$

$$TS_2[i,j] = \sqrt{\frac{1}{NL}\sum_{k=1}^{N}\sum_{l=1}^{L}\left(\frac{Q_k(T_l) - \widehat{Q_k}(T_l)}{Q_k(T_l)}\right)^2}, \tag{32}$$

where $Q_k(T_l)$ is the reference flood quantile at site *k*, calculated with the observed flood series and $\widehat{Q_k}(T_l)$ is the estimated flood quantile at site *k*, calculated with the regional approach, (Eq. 1), with regional models $M_R[i,j]$. The quantile RMSE was estimated for each gauging station and for *L*=7 return periods (T_l= 1, 2, 5, 10, 20, 50, and 100 years), and then averaged over all gauging stations (TS_1). For TS_2, the estimation was made over all, (*N*=10), gauging stations and for *L*=4 return periods (T_l=10, 20, 50, and 100 years).

Figures 11 and 12 present the TS_1 and TS_2 scores which summarize the overall quality of the estimated flood frequency distributions. Appendix 2 presents the observed and simulated flood frequency distributions obtained for each delineation method with the overall best index flood model (see Figs. 7 to 10), and then the best overall regional model, with respect to the TS_2 statistics (see Fig. 12). The error depends both on the quality of the index flood estimation and on the regional growth curve estimation. It was observed that the best results were often, but not systematically, obtained with the overall best index flood estimation model or close to the best one, because of compensating errors such as an over- (under-) estimation of the regional growth factor and an under- (over-) estimation of the index flood. The growth curves were usually well estimated and the main difficulty for estimating the flood frequency curve at ungauged catchments was related to the quality of the index flood estimation at the "ungauged" catchment. An under- or over-estimation of the catchment index flood had the strongest impact on the estimated flood frequency distribution, even when the regional growth curve was rather well estimated and representative of the catchment of interest.

The lowest overall TS_1 score was obtained with $M_R[3,5]$ and the lowest overall TS_2 score was observed with $M_R[5,3]$ but was not very different from $M_R[1,2:5]$ or $M_R[2,2:5]$ nor from $M_R[3,3:4]$ or $M_R[5,2:4]$. For all *DHR* methods, the lowest TS_2 score was always observed with $REM[3]$. It was also observed that when the index flood of the catchment was rather well estimated and unbiased, the estimated quantiles were within the 95% confidence interval of the reference distribution (grey region), and vice-versa, the reference quantiles were within the estimated 95% confidence interval (green dashed lines in figures of Appendix 2). The cluster delineation method used with set_2, ($DHR[4]$) gave usually the worst results, although the same distance metric was used with both clustering and ROI delineation methods.

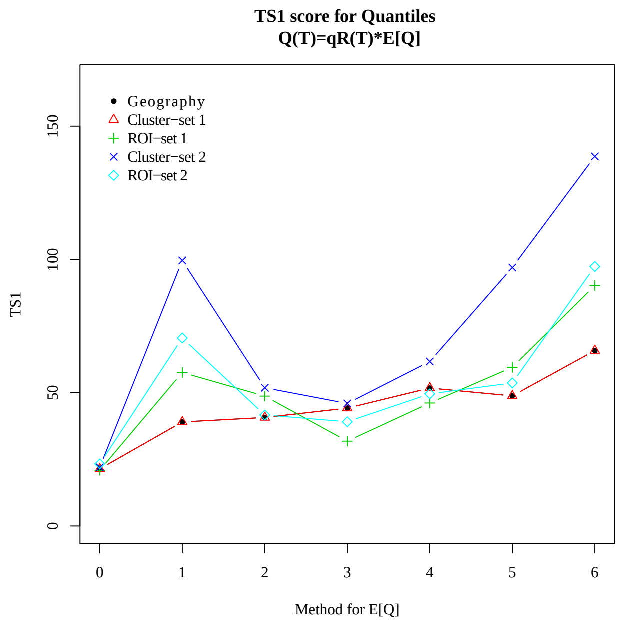

Figure 11. TS_1 score versus regional estimation method (REM). $REM[1:6]$ correspond to the index flood estimation made by Eqs. (23–28) and $REM[0]$ is the reference estimation, given by the observed sample mean.

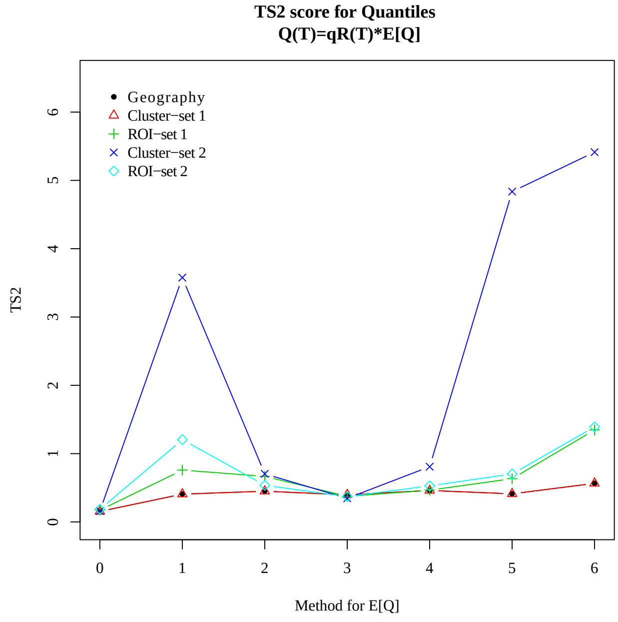

Figure 12. TS_2 score (bottom) versus regional estimation method (REM). $REM[1:6]$ correspond to the index flood estimation made by Eqs. (23–28) and $REM[0]$ is the reference estimation, given by the observed sample mean.

5 Conclusion and future research

The regional flood frequency analysis presented in this study was shown to be a powerful tool for estimating the flood frequency distribution and calculating the T-year flood and its confidence interval at poorly gauged and ungauged natural catchments. Care must be taken when identifying homogeneous groups of watersheds and the objective delineation strategies tested for performing this task proved to be useful. The selection of the best index flood model appeared to be crucial for the method. A poor estimate of the catchment index flood may lead to severe under- or over-estimation of the flood frequency distribution even though the regional growth curve is well estimated. The results indicated that the two objective delineation techniques should be used rather than a geographic delineation as they allowed to obtain similar and sometimes better results in a rational and objective manner. These results also indicated that the geographic regions defined in Crochet (2012a) were reasonably well chosen.

6 Acknowledgements

This study was supported by Vegagerðin (the Icelandic Road Administration).

7 References

Burn, D.H. (1990a). An appraisal of the "region of influence" approach to flood frequency analysis. Hydrol. Sci. J., 35 (2), 149–165.

Burn, D.H. (1990b). Evaluation of regional flood frequency analysis with a region of influence approach. Water Resour. Res., 26(10), 2257–2265.

Crochet, P., Jóhannesson, T., Jónsson, T., Sigurðsson, O., Björnsson, H., Pálsson, F. & Barstad, I. (2007). Estimating the spatial distribution of precipitation in Iceland using a linear model of orographic precipitation. J. Hydrometeorol., 8, 1285–1306.

Crochet, P. & Jóhannesson, T. (2011). A dataset of daily temperature in Iceland for the period 1949–2010. Jökull, 61, 1–17.

Crochet, P. (2012a). Estimating the flood frequency distribution for ungauged catchments using an index flood procedure. Application to ten catchments in Northern Iceland. Icelandic Met. Office report No. VÍ 2012-005, 59pp.

Crochet, P. (2012b). Hydrologic sensitivity of Icelandic river basins to recent climatic variations. Submitted.

Dalrymple, T. (1960). Flood frequency analysis. US Geol. Surv. Water Supply Paper, 1543 A.

Das, S. & Cunnane, C. (2011). Examination of homogeneity of selected Irish pooling groups. Hydrol. Earth Sys. Sci., 15, 819–830.

GREHYS. (1996a). Presentation and review of some methods for regional flood frequency analysis. J. Hydrol., 186, 63–84.

GREHYS. (1996b). Inter-comparison of regional flood frequency procedures for Canadian rivers. J. Hydrol., 186, 85–103.

Grover, P.L., Burn, D.H. & Cunderlik, J.M. (2002). A comparison of index flood estimation procedures for ungauged catchments. Can. J. Civ. Eng., 29, 731–741.

Hosking, J.R.M, Wallis, J.R. & Wood, E.F. (1985a). Estimation of the generalized extreme-value distribution by the method of the probability-weighted moments. Technometrics, 27(3), 251–261.

Hosking, J.R.M, Wallis, J.R. & Wood, E.F. (1985b). An appraisal of the regional flood frequency procedure in the UK Flood Studies Report. Hydrol. Sci. J., 30, 85–109.

Hoskings, J.R.M. & Wallis, J.R. (1993). Some statistics useful in regional frequency analysis. Water. Resour. Res. 29, 271-281.

Jenkinson, A.F. (1955). The frequency distribution of the annual maximum (or minimum) of meteorological elements. Quart. J. R. Met. Soc. 81, 158–171.

Jingyi, Z. & Hall, M.J. (2004). Regional flood frequency analysis for Gan-Ming river basin in China. J. Hydrol., 296, 98–117.

Lu, L.H. & Stedinger, J.R. (1992). Variance of two- and three-parameter GEV/PWM quantile estimators: formulae, confidence intervals and a comparison. J. Hydrol., 138, 247-267.

Malekinezhad, H., Nachtnebel, H.P. & Klik, A. (2011a). Comparing the index flood and multiple-regression methods using L-moments. J. Phys. Chem. Earth, 36, 54–60.

Malekinezhad, H., Nachtnebel, H.P. & Klik, A. (2011b). Regionalization approach for extreme flood analysis using L-moments. J. Agr. Sci. Tech., 13, 1183–1196.

Stedinger, J.R., Vogel, R.M. & Foufoula-Georgiou, E. (1992). Frequency analysis of extreme events. Handbook of Hydrology, D.R. Maidmment Ed., McGraw-Hill.

Appendix 1

Regional growth curves obtained for each watershed using the ROI delineation method with the first set of attributes, set_1**. The experimental and modeled GEV growth curves for the target (or reference) watershed and all watersheds defining its ROI are also presented.**

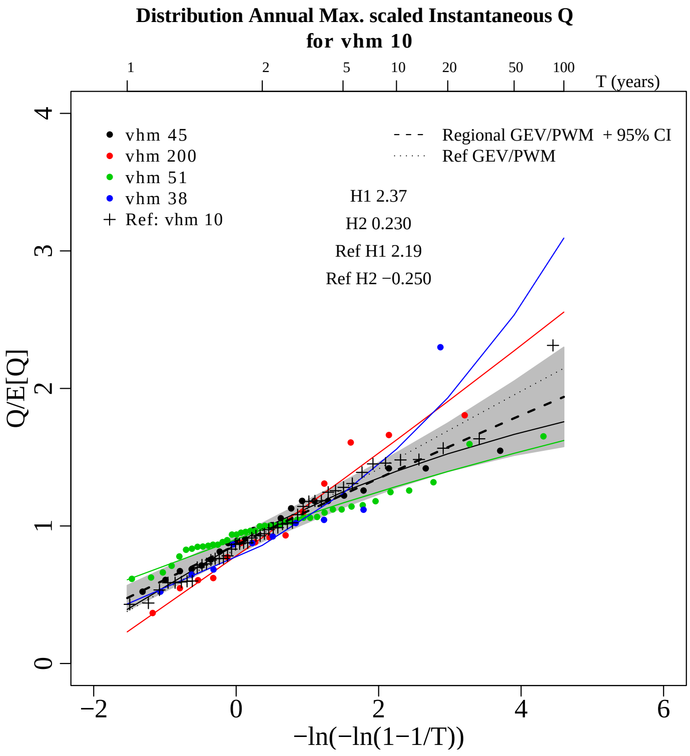

Figure I.1.

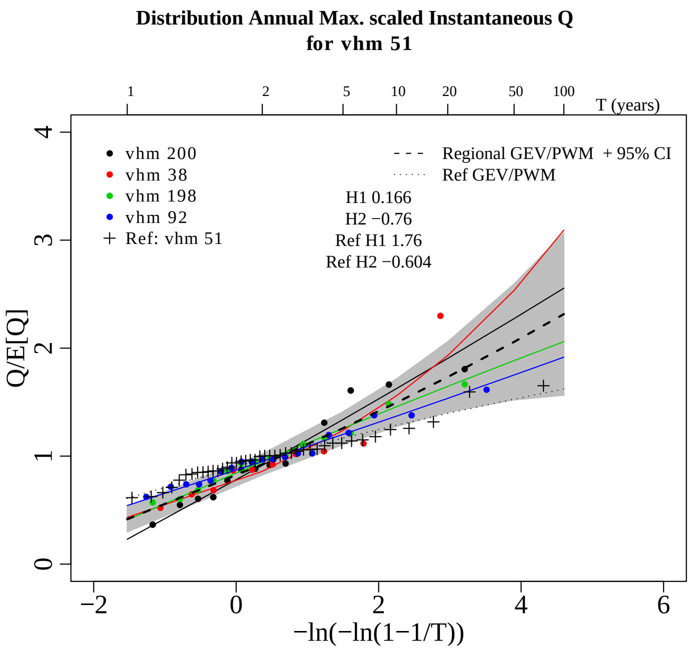

Figure I.2.

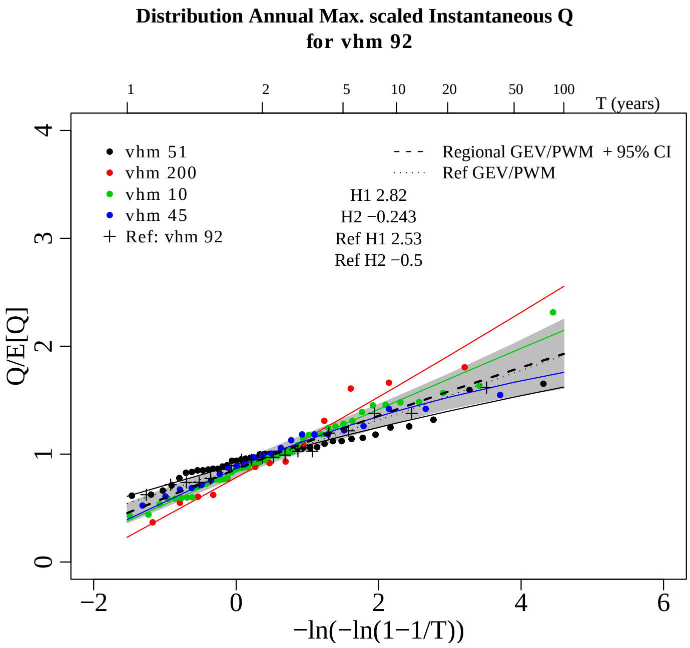

Figure I.3.

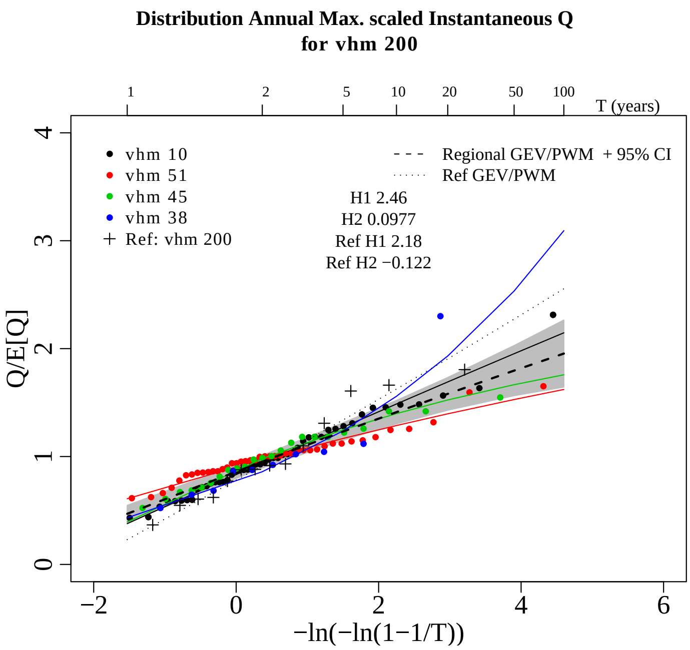

Figure I.4.

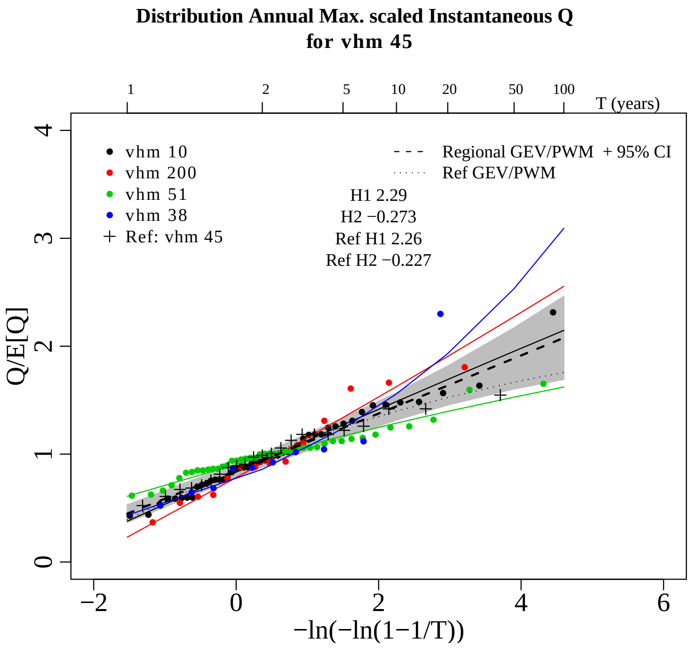

Figure I.5.

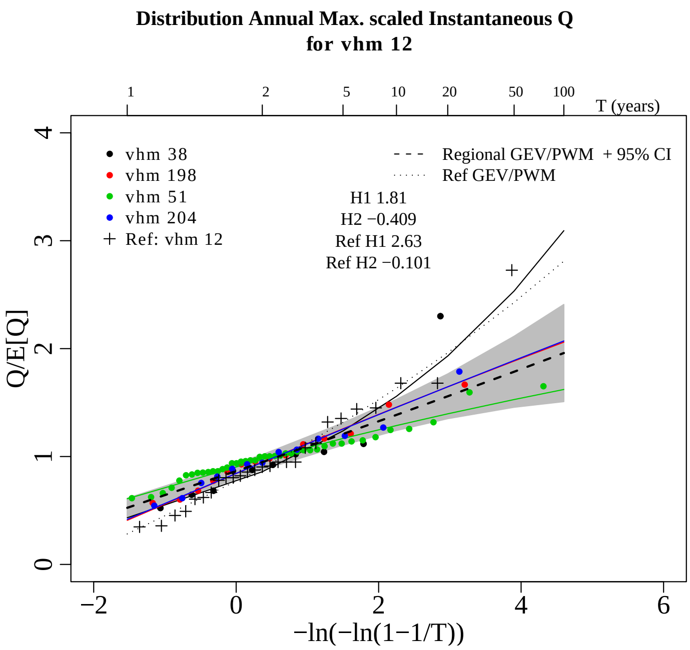

Figure I.6.

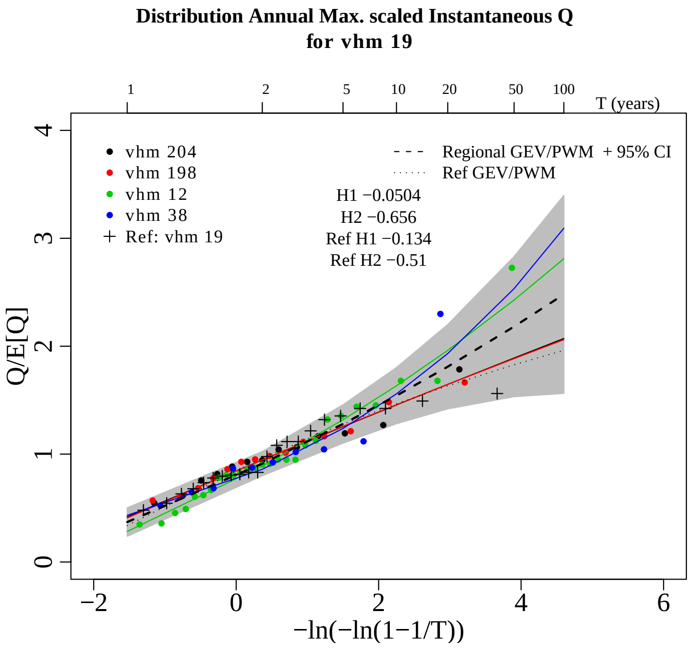

Figure I.7.

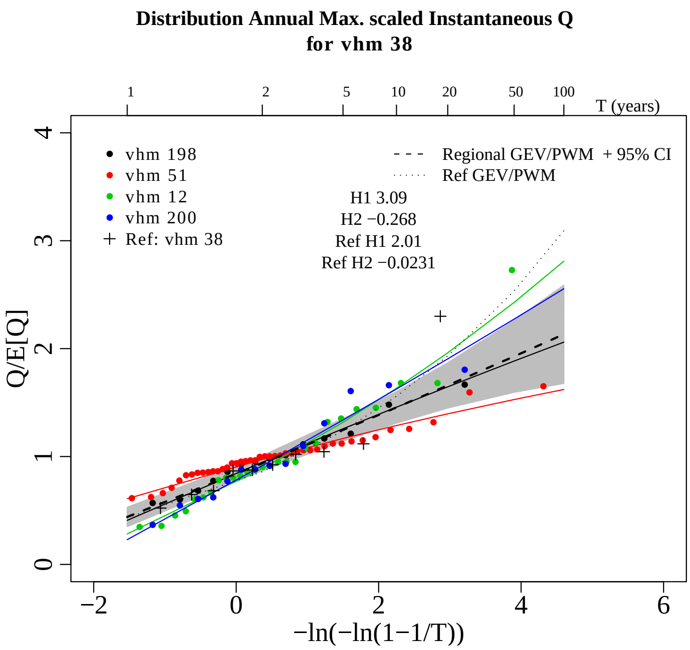

Figure I.8.

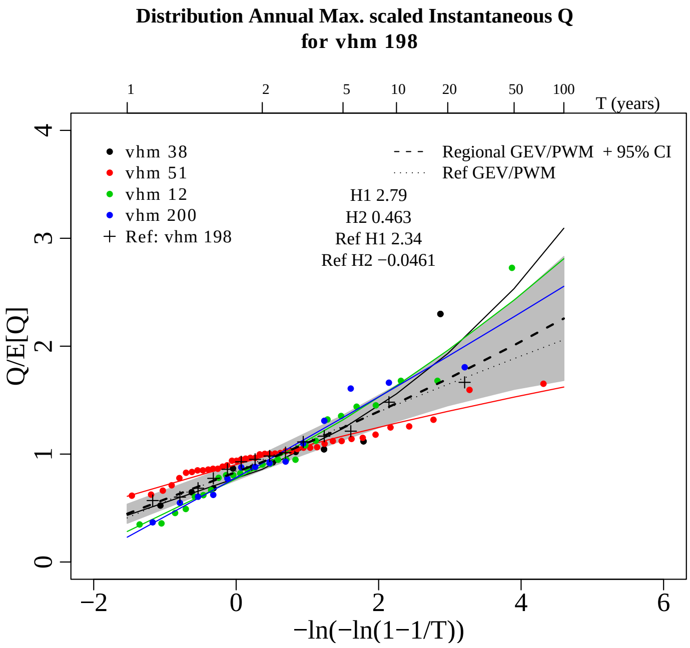

Figure I.9.

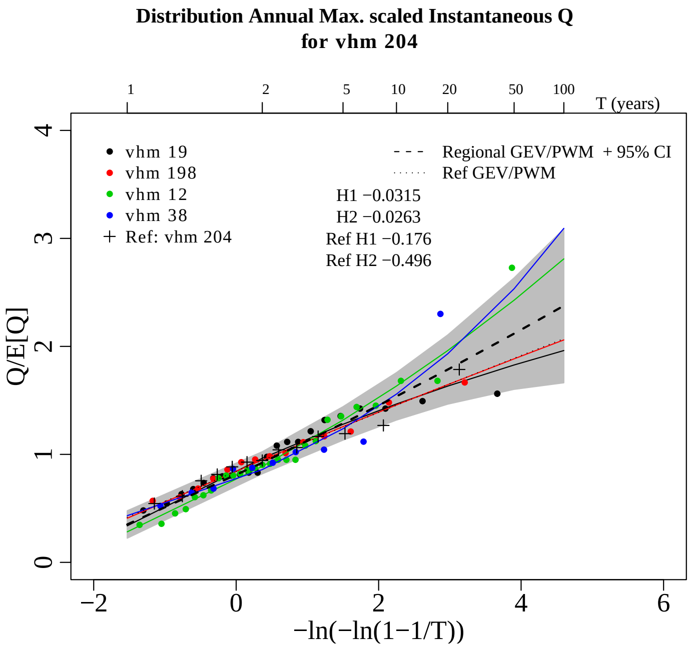

Figure I.10.

Appendix 2

Annual maximum instantaneous flood cumulative distribution functions (CDFs), derived with the regional flood frequency analysis, using three different delineation methods and six different index flood models.

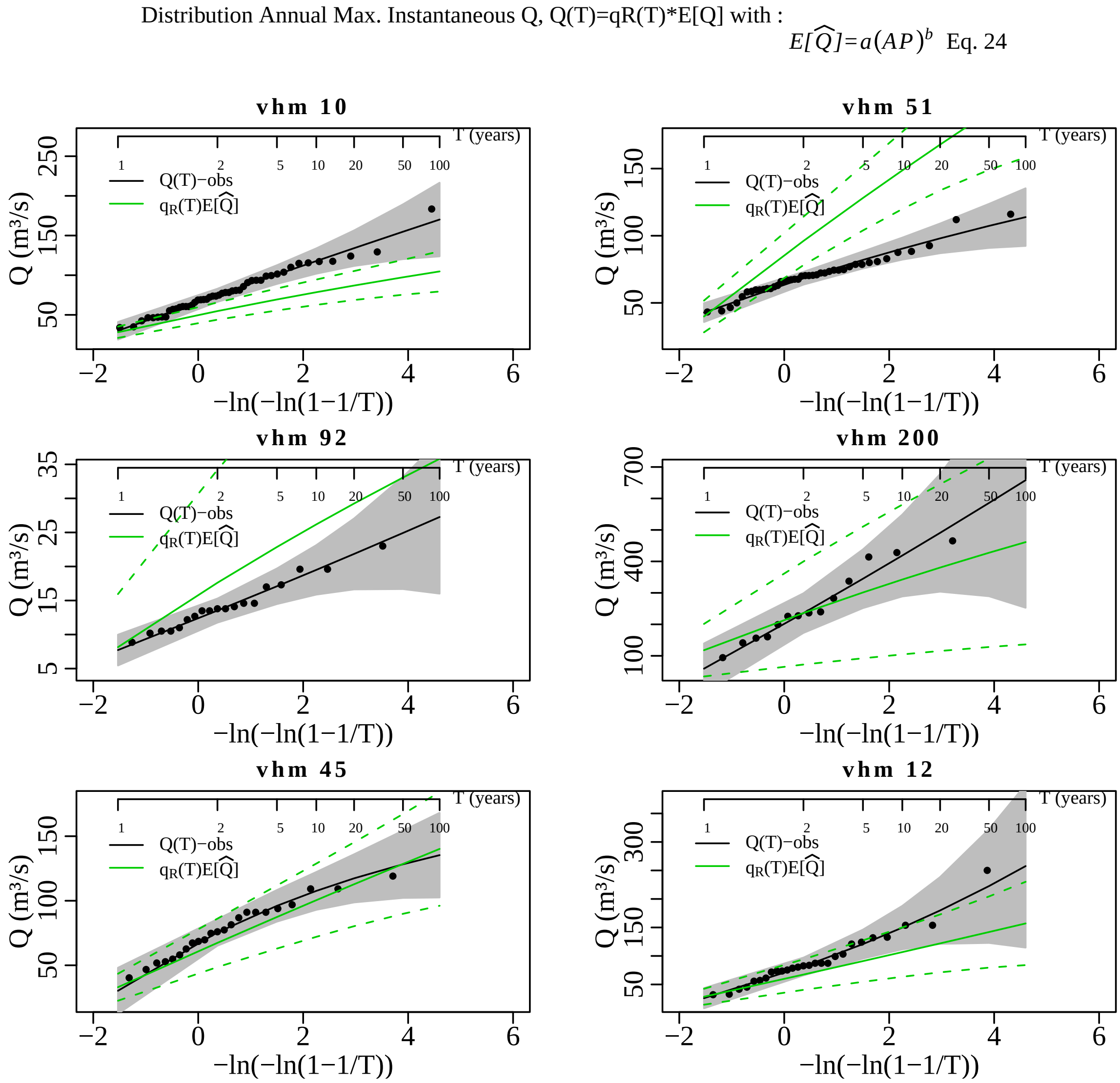

Figure II.1. Flood frequency distribution using the geographic delineation method with overall best index flood model (Eq. 24). The black dots correspond to the empirical distribution and the black line corresponds to the adjusted GEV distribution (reference). The corresponding 95% confidence interval is defined by the grey shaded region. The estimated distribution using the regional flood frequency procedure is given by the solid green line and its 95% confidence interval is given by the dashed green lines.

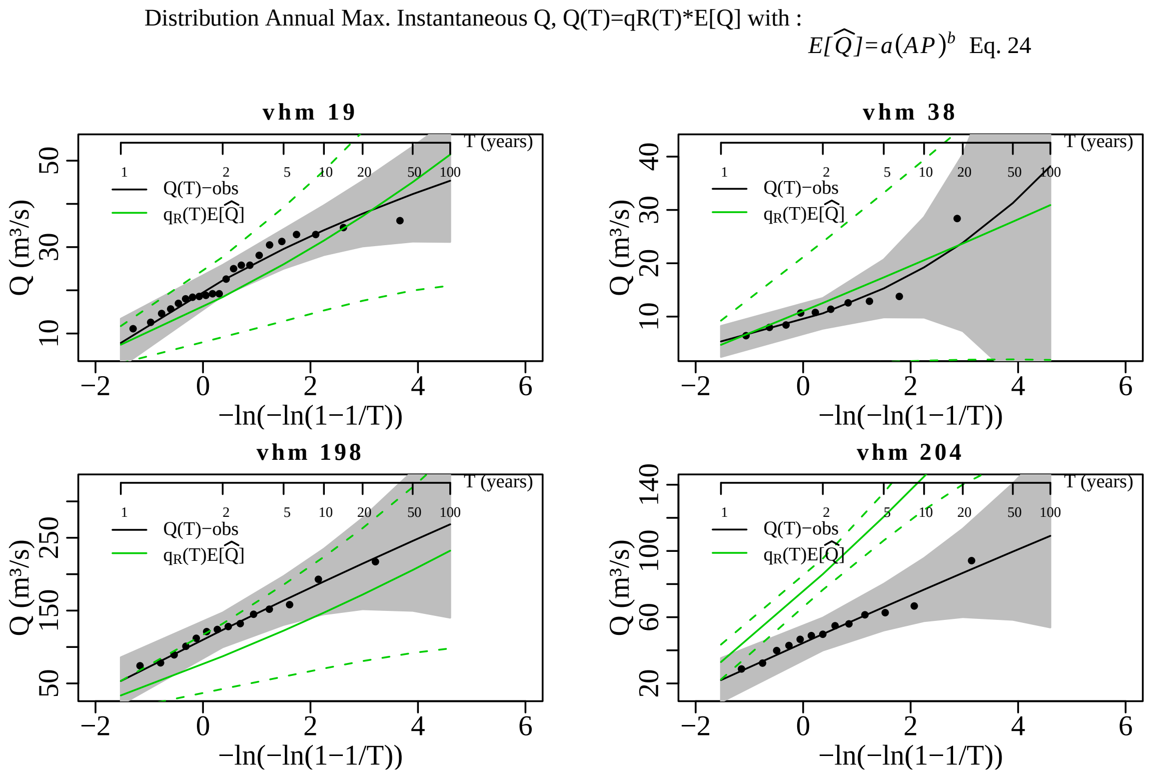

Figure II.2. Flood frequency distribution using the geographic delineation method with overall best index flood model (Eq. 24).

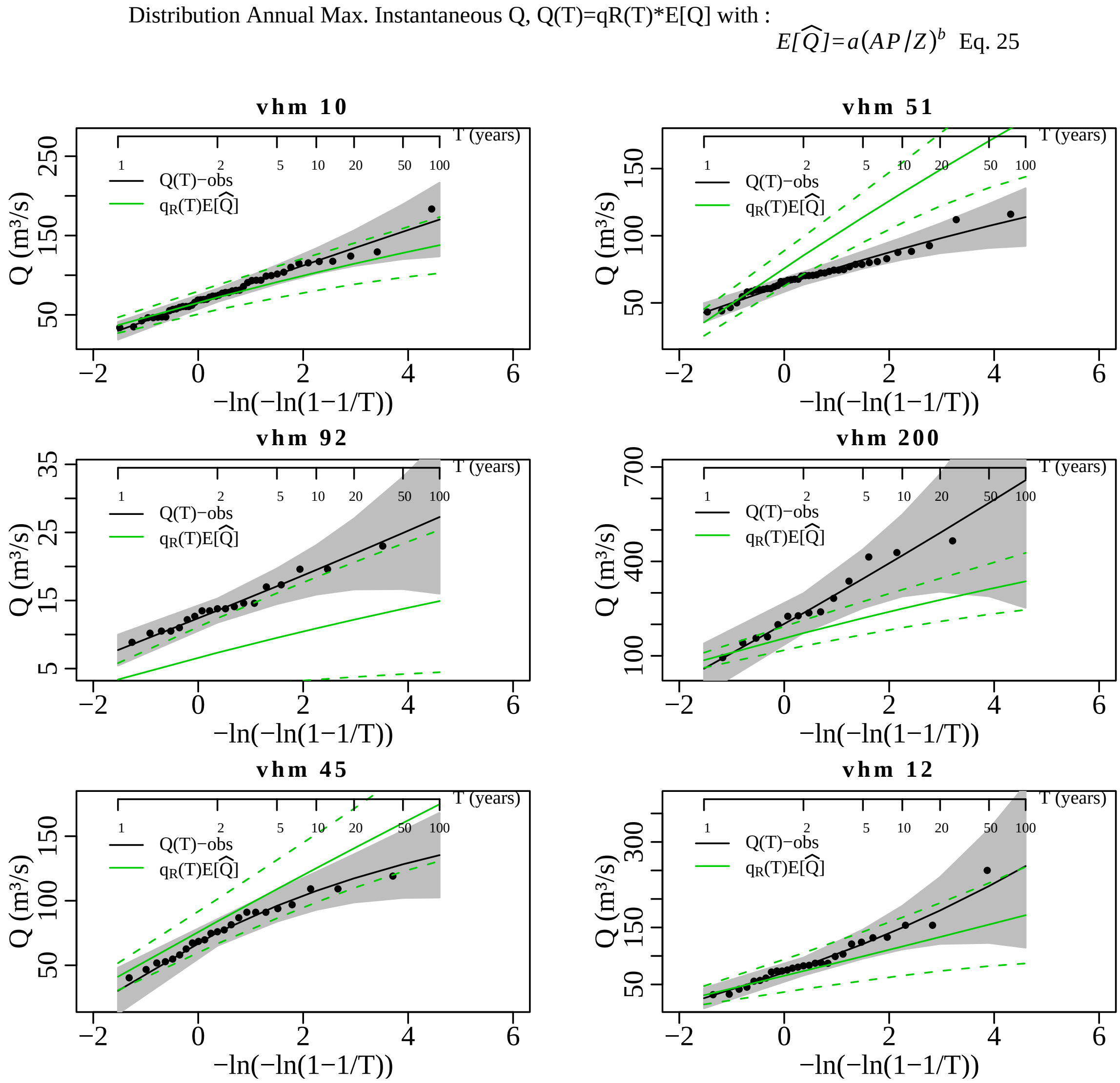

Figure II.3. Flood frequency distribution using the geographic delineation method and index flood model giving lowest TS_2 score (Eq. 25). The black dots correspond to the empirical distribution and the black line corresponds to the adjusted GEV distribution (reference). The corresponding 95% confidence interval is defined by the grey shaded region. The estimated distribution using the regional flood frequency procedure is given by the solid green line and its 95% confidence interval is given by the dashed green lines.

Distribution Annual Max. Instantaneous Q, Q(T)=qR(T)*E[Q] with :

$E[\widehat{Q}]=a(AP/Z)^b$ Eq. 25

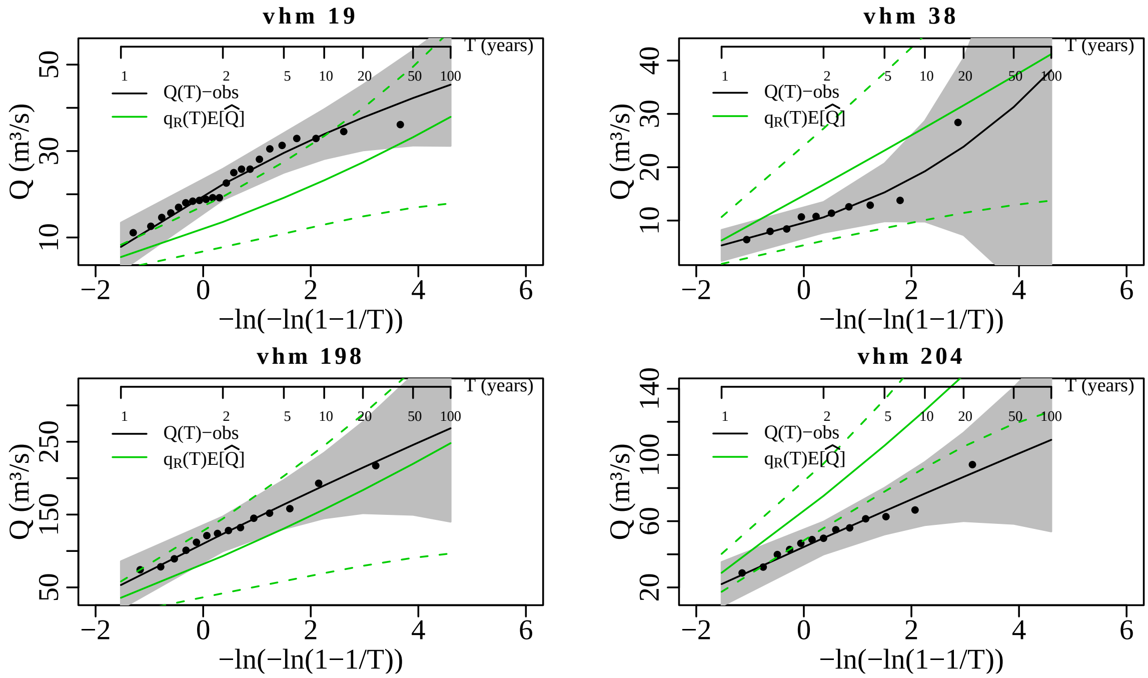

Figure II.4. Flood frequency distribution using the geographic delineation method and index flood model giving lowest TS_2 score (Eq. 25).

ROI: Distribution Annual Max. Instantaneous Q, Q(T)=qR(T)*E[Q] with : $E[\widehat{Q}]=a(Q_s/Z)^b$ Eq. 26

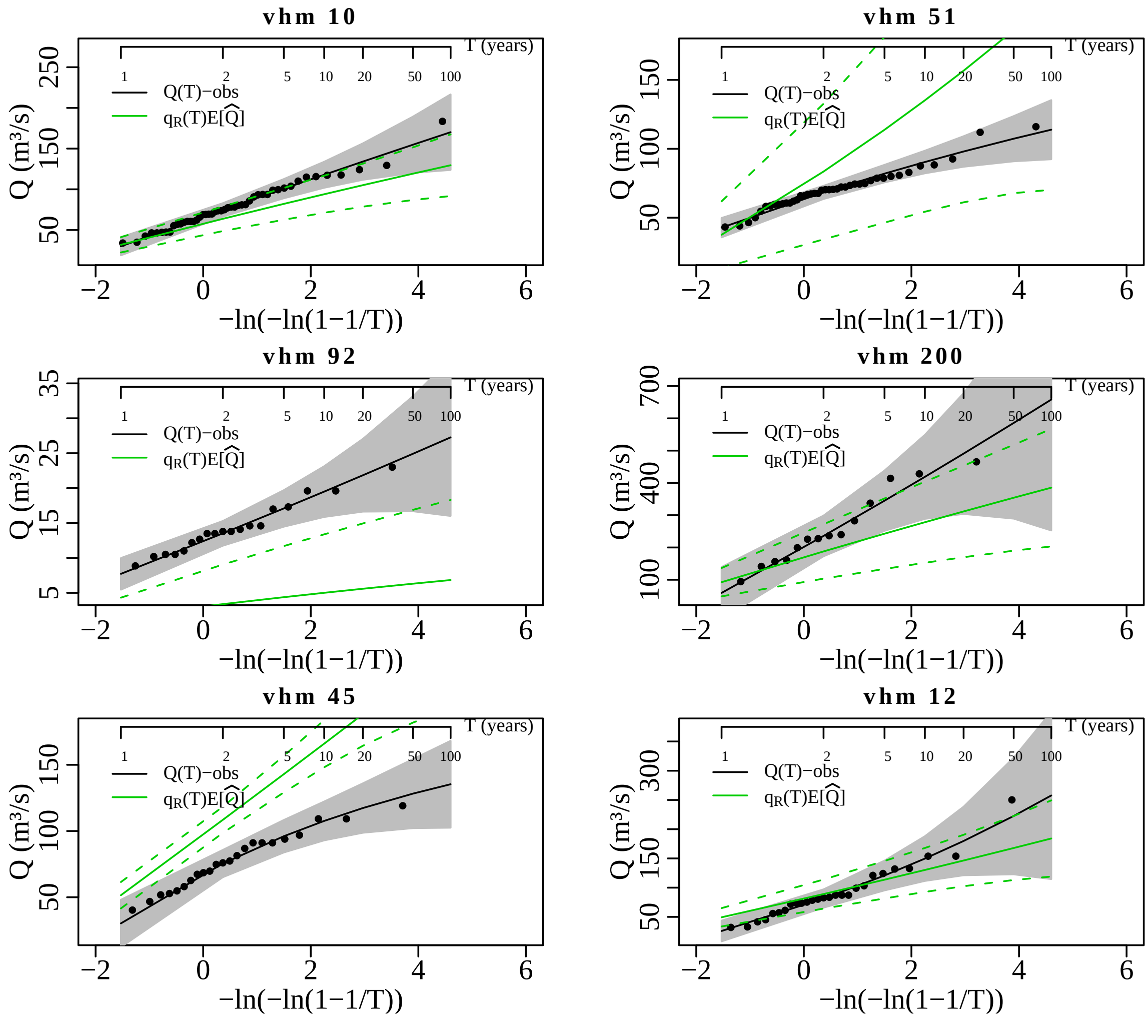

Figure II.5. Flood frequency distribution using the ROI delineation method with first set of attributes set_1 and overall best index flood model (Eq. 26). The black dots correspond to the empirical distribution and the black line corresponds to the adjusted GEV distribution (reference). The corresponding 95% confidence interval is defined by the grey shaded region. The estimated distribution using the regional flood frequency procedure is given by the solid green line and its 95% confidence interval is given by the dashed green lines.

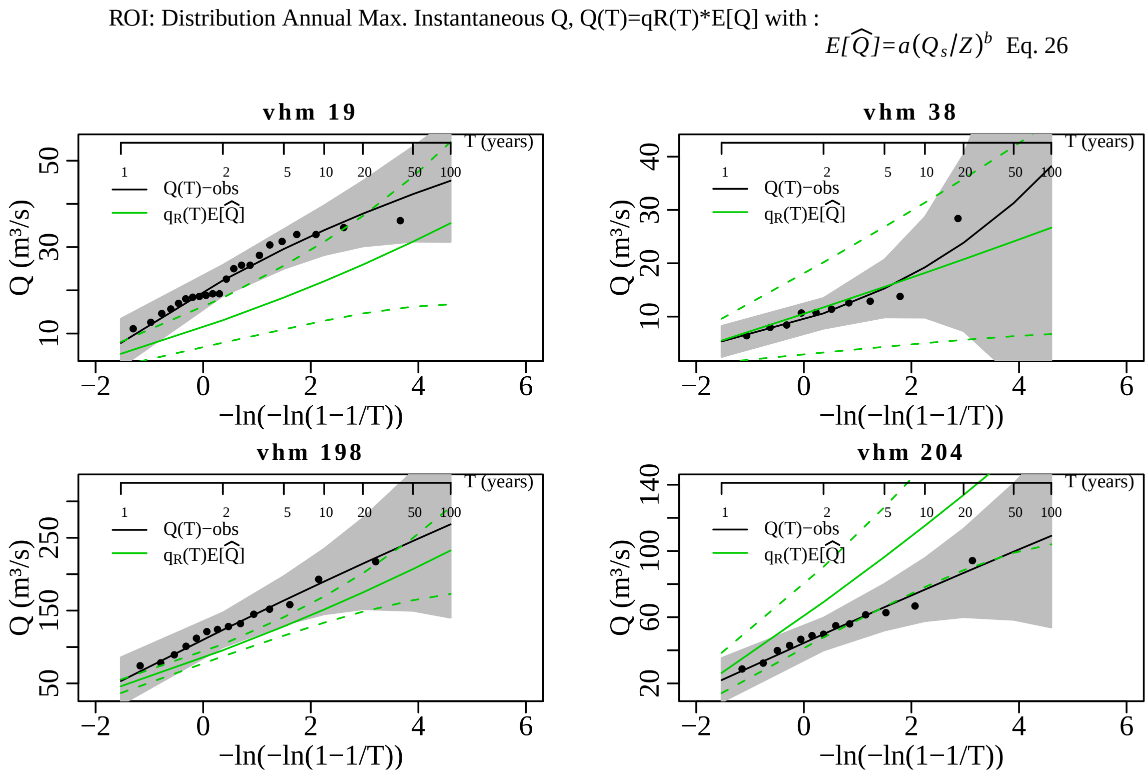

Figure II.6. Flood frequency distribution using the ROI delineation method with first set of attributes set$_1$ and overall best index flood model (Eq. 26).

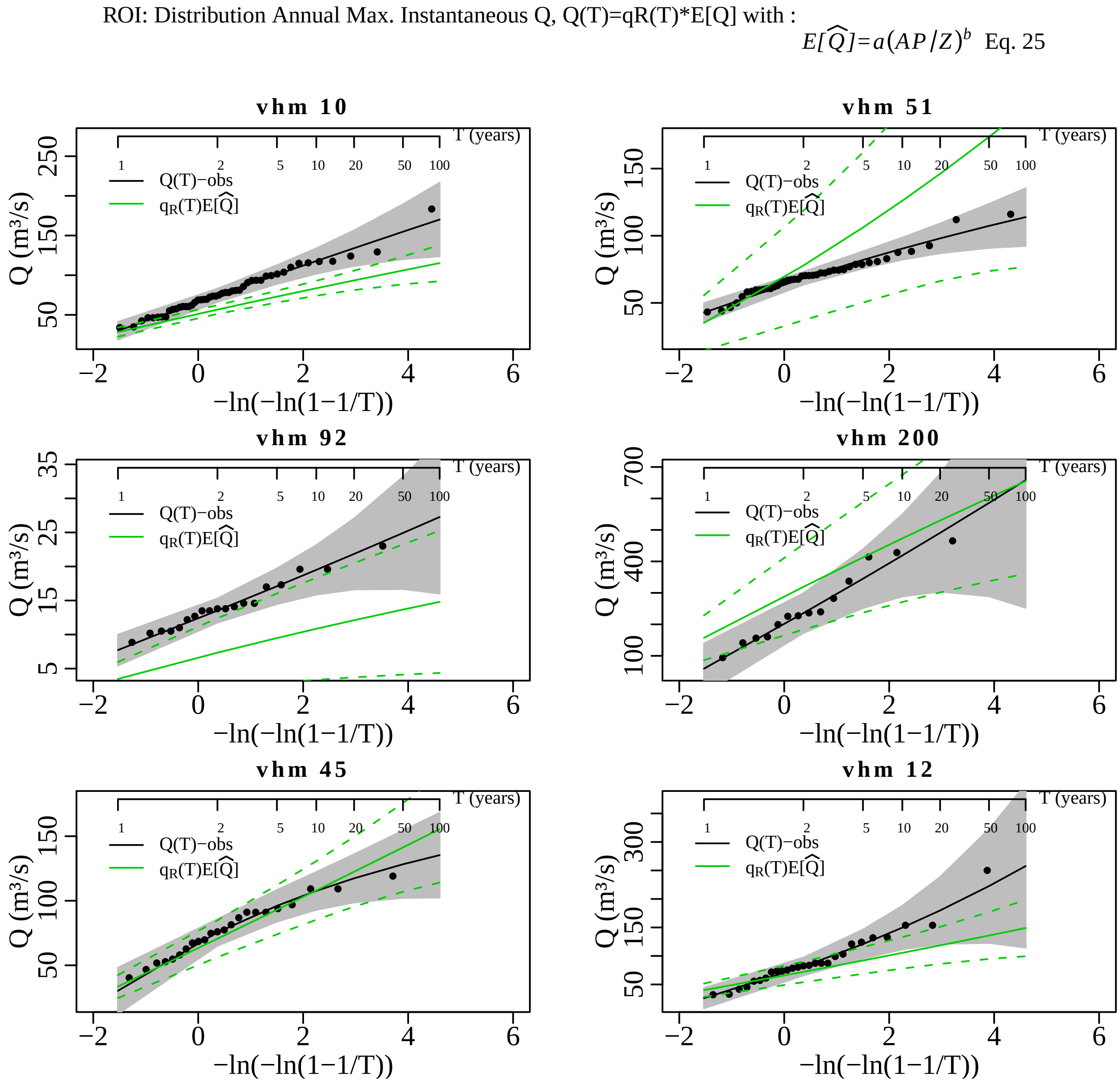

Figure II.7. Flood frequency distribution using the ROI delineation method with first set of attributes set_1 and the index flood model giving lowest TS_2 score (Eq. 25). The black dots correspond to the empirical distribution and the black line corresponds to the adjusted GEV distribution (reference). The corresponding 95% confidence interval is defined by the grey shaded region. The estimated distribution using the regional flood frequency procedure is given by the solid green line and its 95% confidence interval is given by the dashed green lines.

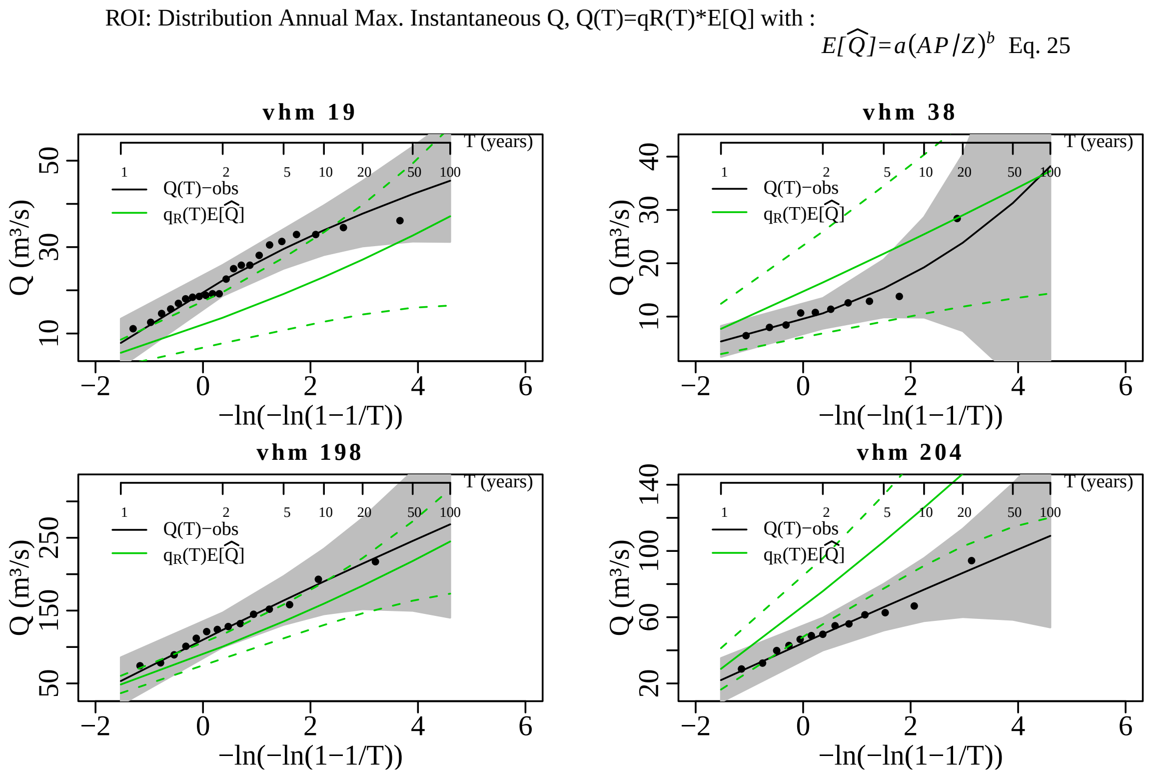

Figure II.8. Flood frequency distribution using the ROI delineation method with first set of attributes set$_1$ and the index flood model giving lowest TS_2 score (Eq. 25).

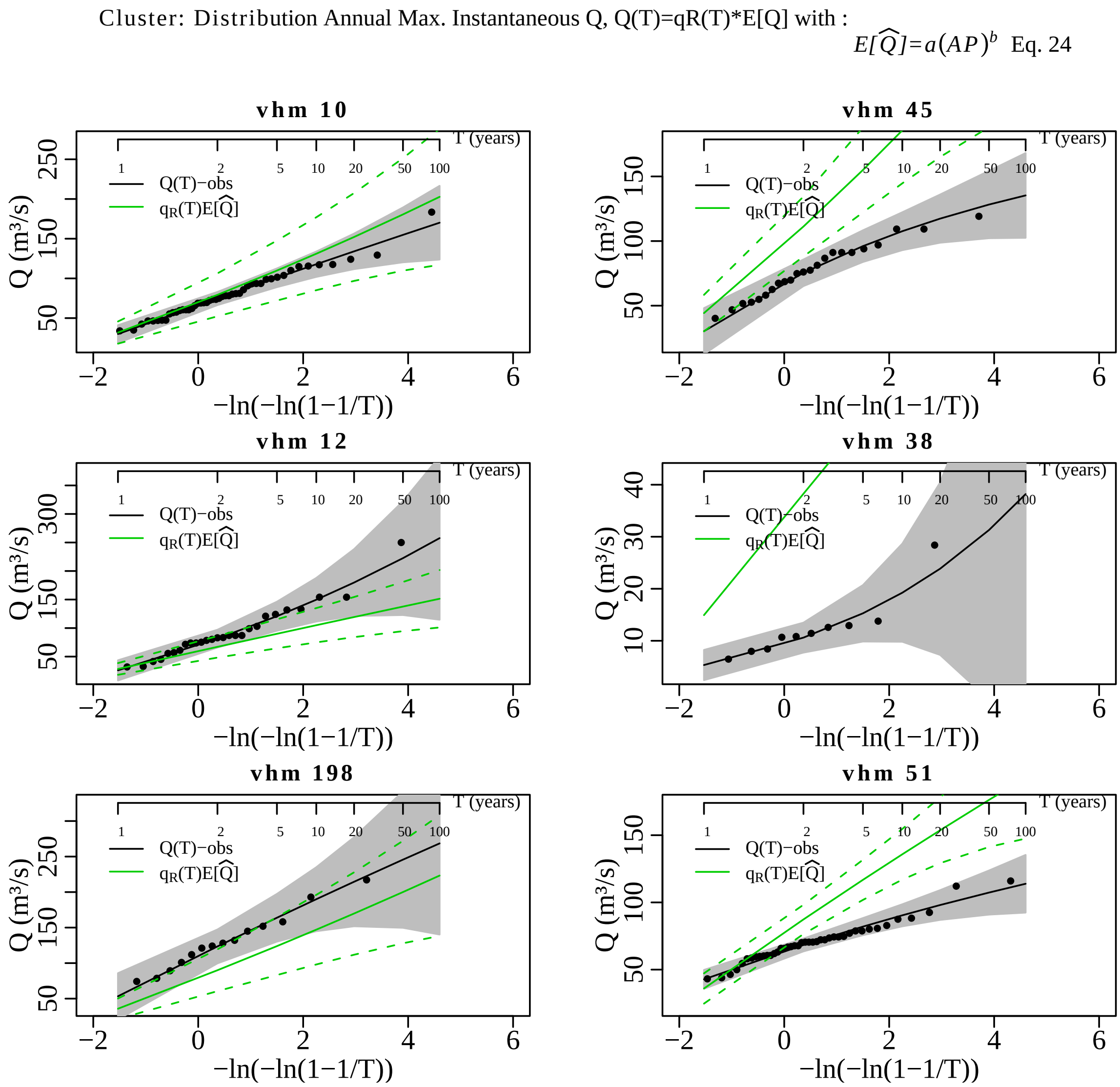

Figure II.9. Flood frequency distribution using the cluster delineation method with second set of attributes set$_2$ and overall best index flood model (Eq. 24). The black dots correspond to the empirical distribution and the black line corresponds to the adjusted GEV distribution (reference). The corresponding 95% confidence interval is defined by the grey shaded region. The estimated distribution using the regional flood frequency procedure is given by the solid green line and its 95% confidence interval is given by the dashed green lines.

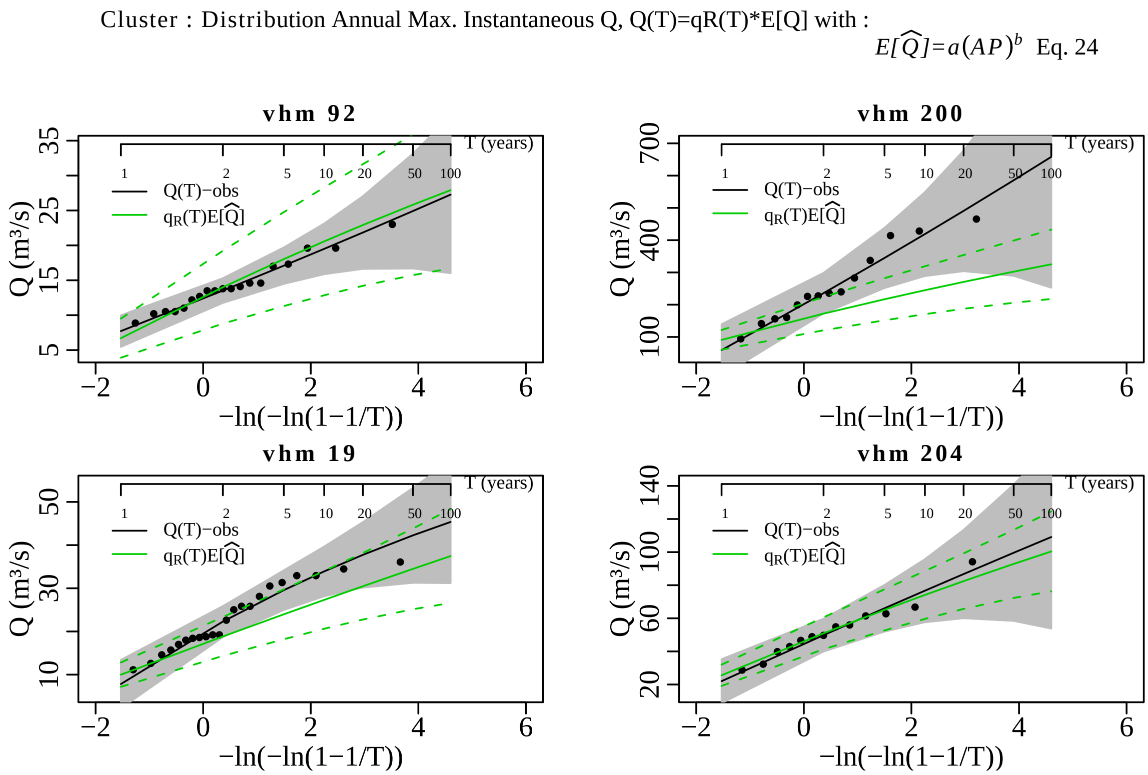

Figure II.10. Flood frequency distribution using the cluster delineation method with second set of attributes set$_2$ and overall best index flood model (Eq. 24).

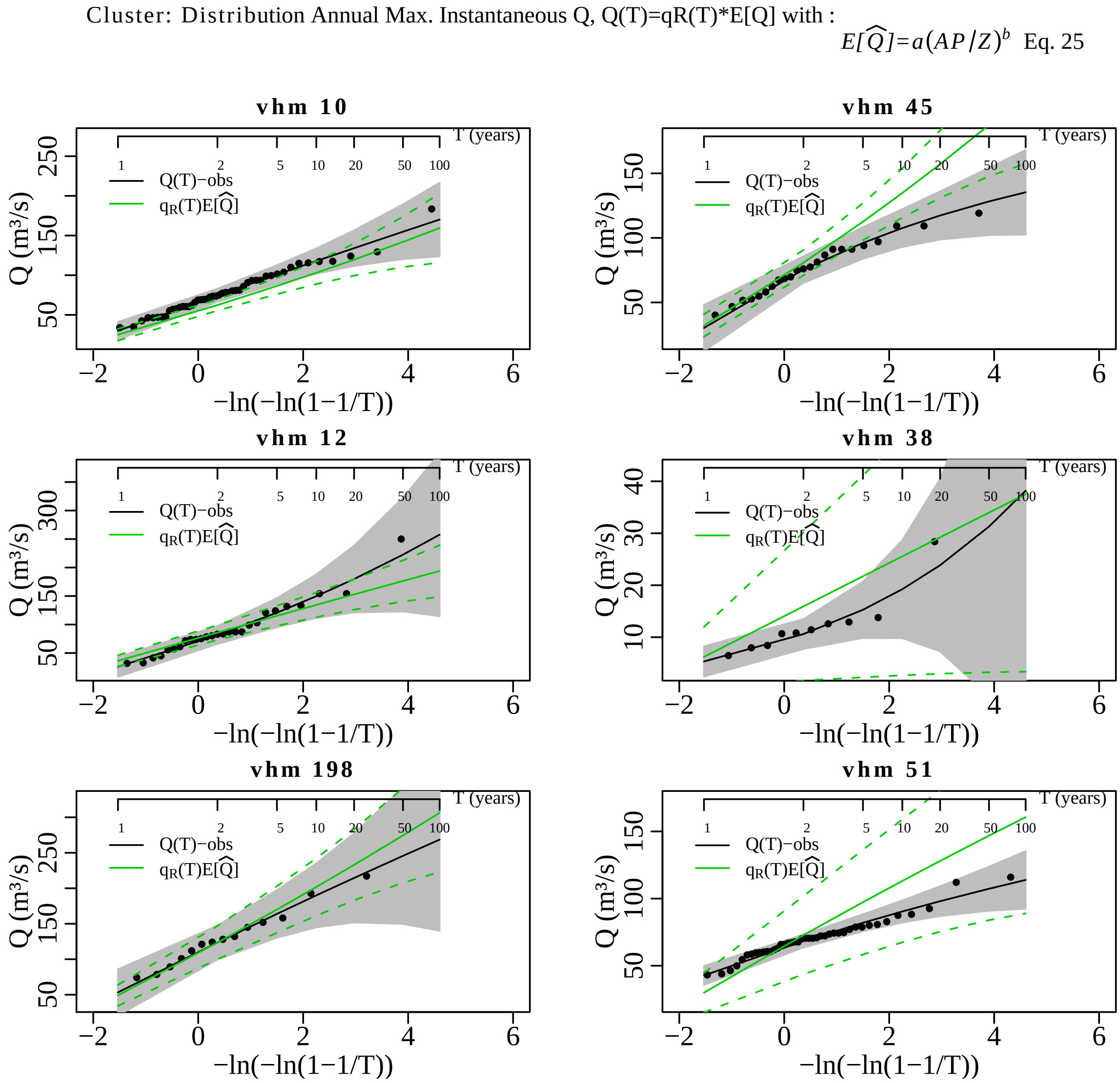

Figure II.11. Flood frequency distribution using the cluster delineation method with second set of attributes set$_2$ and index flood model giving best TS_2 score (Eq. 25). The black dots correspond to the empirical distribution and the black line corresponds to the adjusted GEV distribution (reference). The corresponding 95% confidence interval is defined by the grey shaded region. The estimated distribution using the regional flood frequency procedure is given by the solid green line and its 95% confidence interval is given by the dashed green lines.

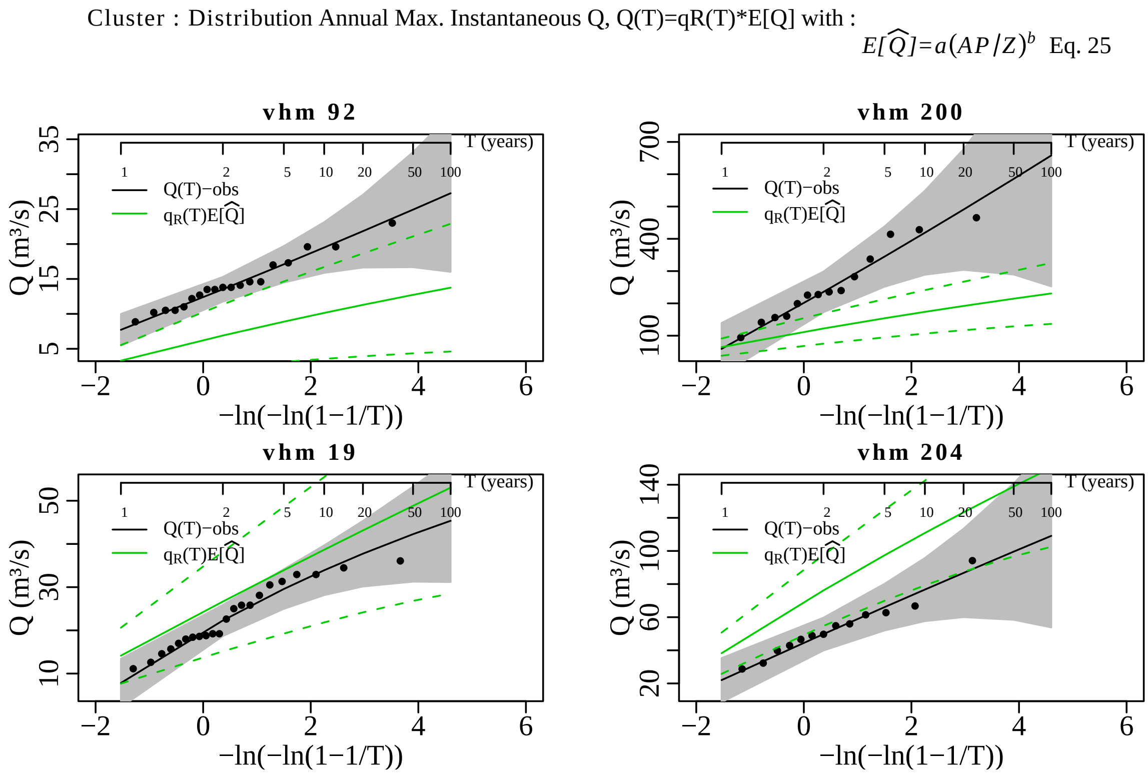

Figure II.12. Flood frequency distribution using the cluster delineation method with second set of attributes set$_2$ and index flood model giving best TS_2 score (Eq. 25).

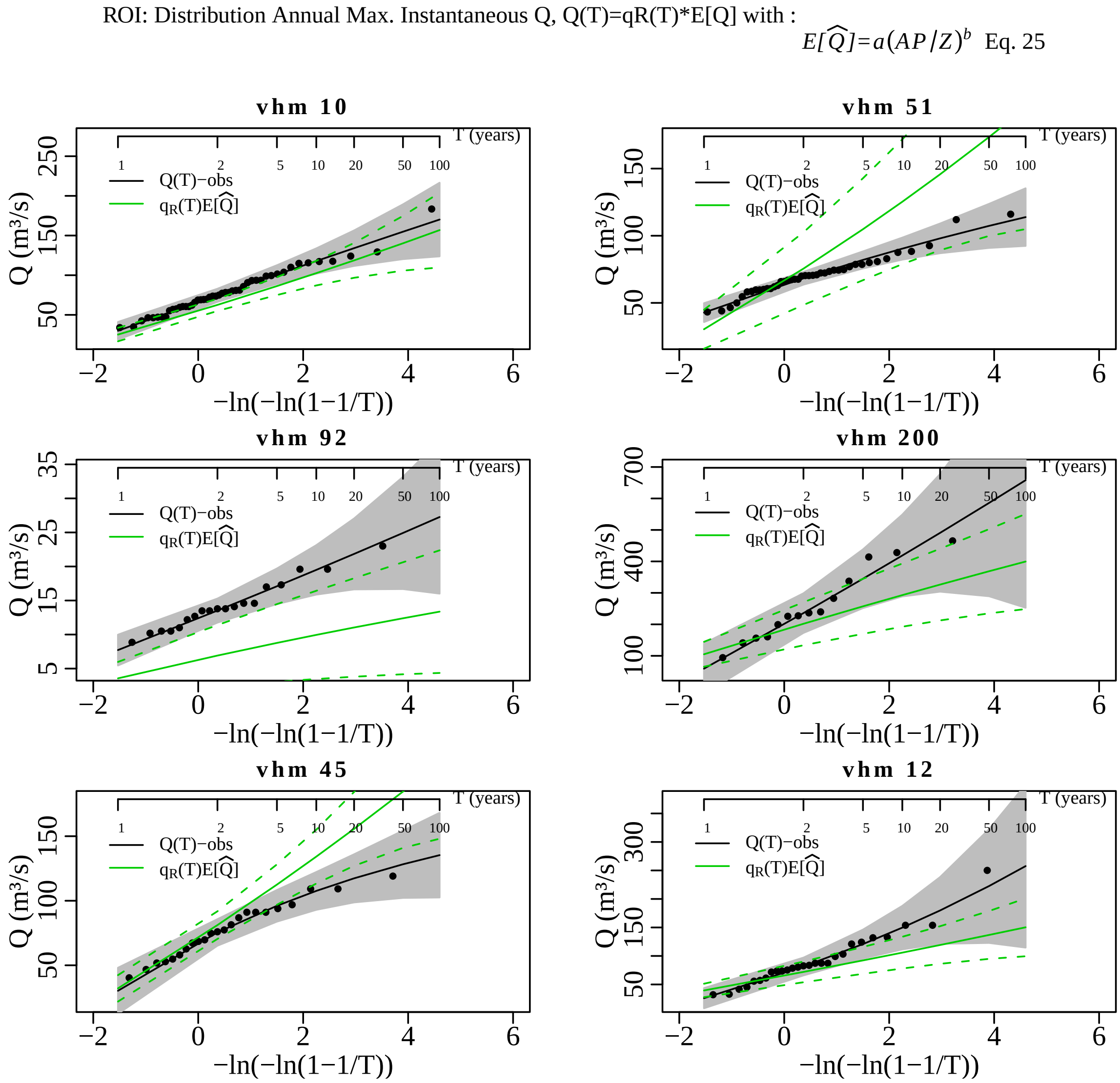

Figure II.13. Flood frequency distribution using the ROI delineation method with second set of attributes set$_2$ and overall best index flood model (Eq. 25). The black dots correspond to the empirical distribution and the black line corresponds to the adjusted GEV distribution (reference). The corresponding 95% confidence interval is defined by the grey shaded region. The estimated distribution using the regional flood frequency procedure is given by the solid green line and its 95% confidence interval is given by the dashed green lines.

ROI: Distribution Annual Max. Instantaneous Q, Q(T)=qR(T)*E[Q] with :

$E[\widehat{Q}]=a(AP/Z)^b$ Eq. 25

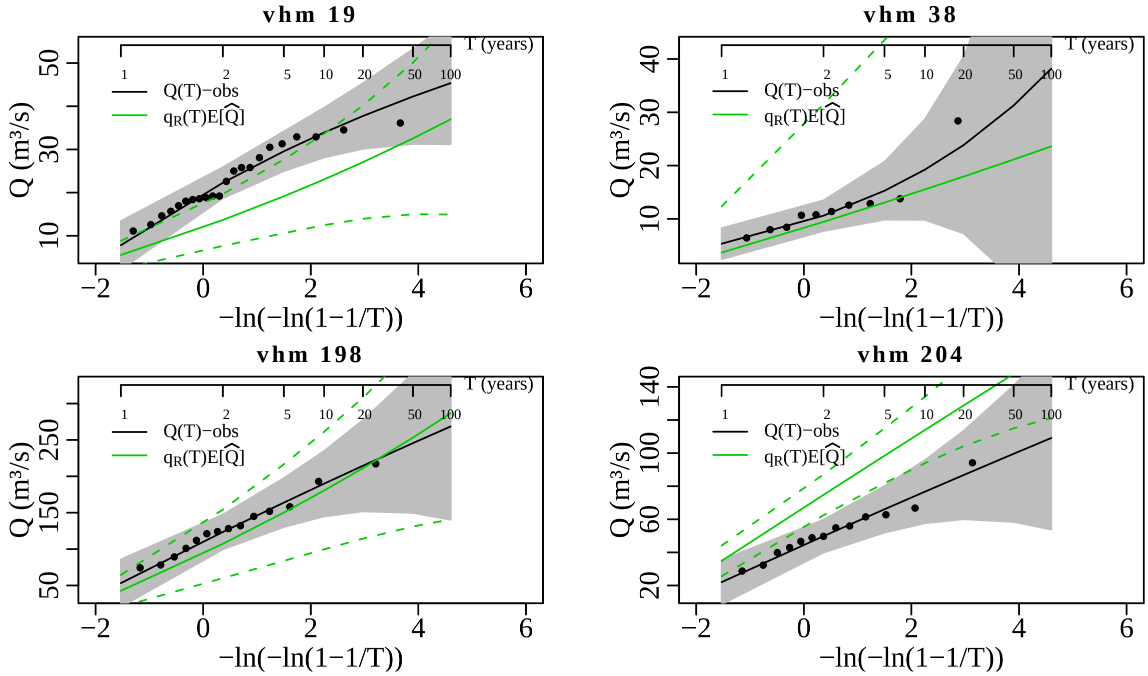

Figure II.14. Flood frequency distribution using the ROI delineation method with second set of attributes set$_2$ and overall best index flood model (Eq. 25).

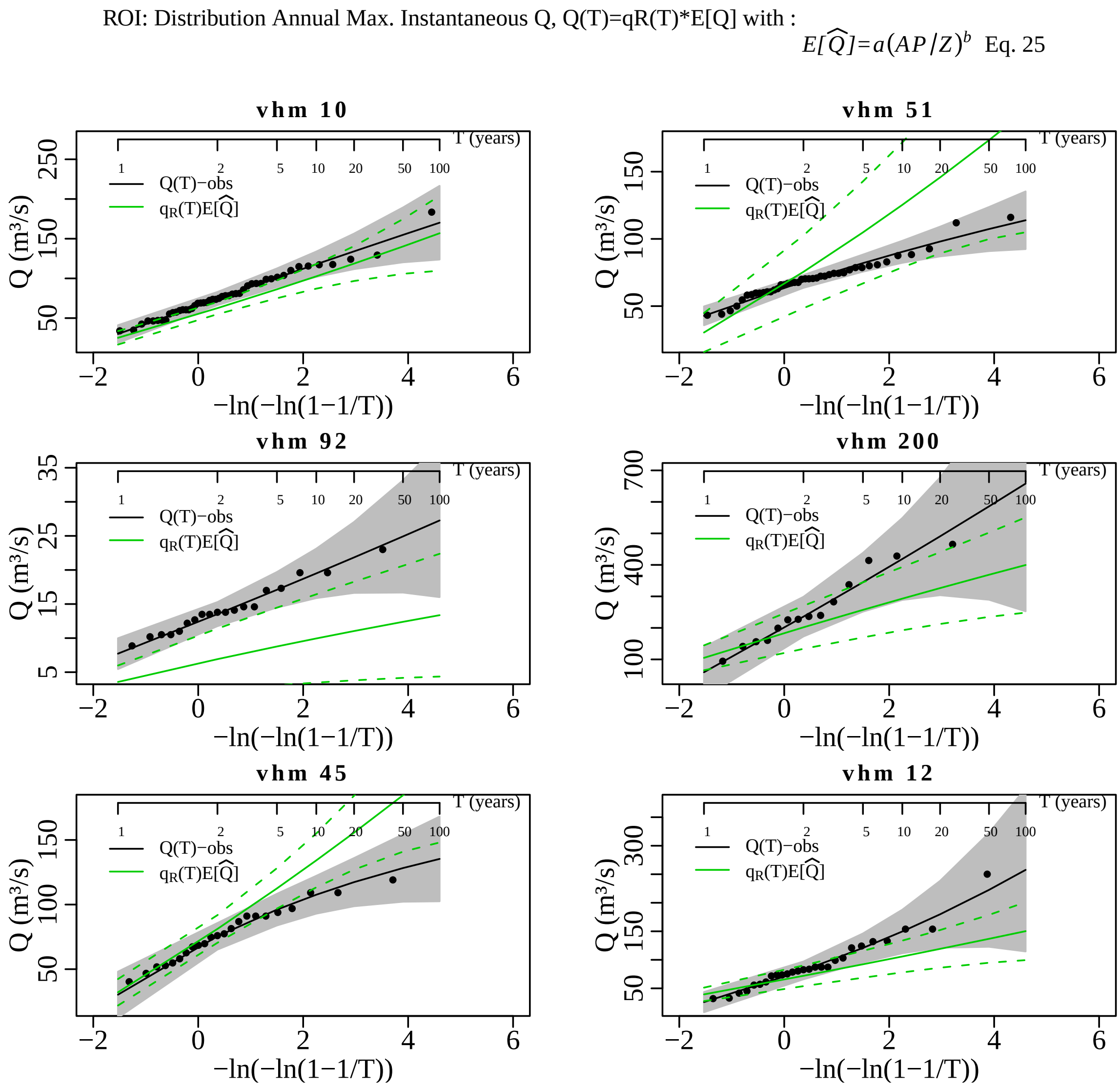

Figure II.15. Flood frequency distribution using the ROI delineation method with second set of attributes set$_2$ and index flood model giving best TS_2 score (Eq. 25). The black dots correspond to the empirical distribution and the black line corresponds to the adjusted GEV distribution (reference). The corresponding 95% confidence interval is defined by the grey shaded region. The estimated distribution using the regional flood frequency procedure is given by the solid green line and its 95% confidence interval is given by the dashed green lines.

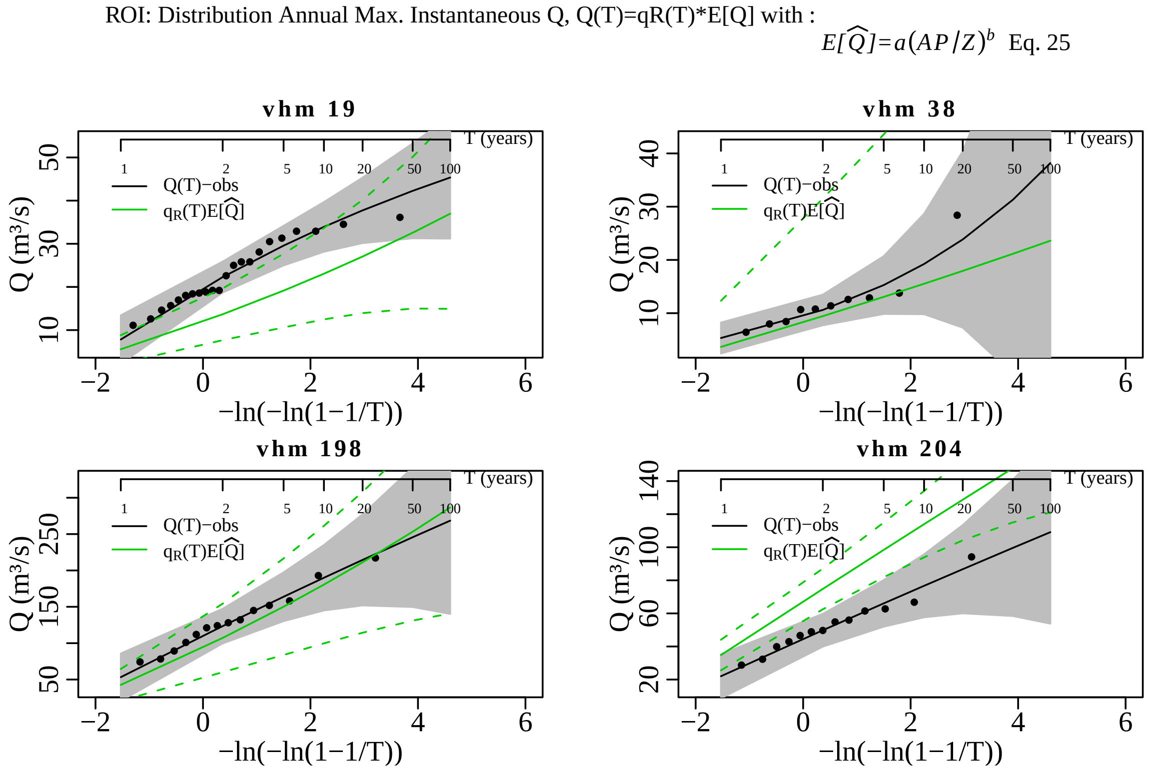

Figure II.16. Flood frequency distribution using the ROI delineation method with second set of attributes set$_2$ and index flood model giving best TS_2 score (Eq. 25).